

# A Reciprocal Formulation of Nonexponential Radiative Transfer. 2: Monte Carlo Estimation and Diffusion Approximation

Eugene d'Eon  
8i

## Abstract

When lifting the assumption of spatially-independent scattering centers in classical linear transport theory, collision rate is no longer proportional to angular flux / radiance because the macroscopic cross-section  $\Sigma_t(s)$  depends on the distance  $s$  to the previous collision or boundary. This creates a nonlocal relationship between collision rate and flux and requires revising a number of familiar deterministic and Monte Carlo methods. We generalize collision and track-length estimators to support unbiased estimation of either flux integrals or collision rates in generalized radiative transfer (GRT). To provide benchmark solutions for the Monte Carlo estimators, we derive the four Green's functions for the isotropic point source in infinite media with isotropic scattering. Additionally, new moment-preserving diffusion approximations for these Green's functions are derived, which reduce to algebraic expressions involving the first four moments of the free-path lengths between collisions.

**Keywords:** generalized radiative transfer, non-classical Boltzmann, diffusion, reciprocity, track-length estimator, non-Beerian

## 1 Introduction

In the study of particle transport [Williams 1971; Davison 1957], light transport [Chandrasekhar 1960; Arridge 1999; Marshak and Davis 2005; Pharr et al. 2016], seismic wave propagation [Sato et al. 2012], heat transfer [Modest 2003], and other fields [Jagers 1975; Duderstadt and Martin 1979], exact solutions of the transport equation are not possible in most cases and estimations based on Monte Carlo and diffusion theory are common. The nascent theory of *generalized radiative transfer* (GRT) extends the transport equation to support spatial correlation between collisions, and this requires Monte Carlo and deterministic methods to be likewise generalized.

This paper presents new methods for estimating collision rates and flux integrals in monoenergetic, time-independent GRT. These methods are organized into three main groups:

- (Section 3) Collision and track-length estimators for piecewise-homogeneous systems in  $\mathbb{R}^d$  with general anisotropic scattering
- (Section 4) Green's functions for the isotropic point source in infinite homogeneous media in  $\mathbb{R}^d$  with isotropic scattering

- (Section 5) Two families of moment-preserving diffusion approximations for the Green's functions in Section 4 plus an additional pair of diffusion approximations for collision rate with a general anisotropic scattering law.

The Monte Carlo estimators and Green's functions are presented together in order to cross-validate each other, and the diffusion approximations follow directly from the Green's functions. All of the methods reduce to familiar forms in the classical case of no correlation and are all motivated by two unique properties of nonclassical transport: nonlocal interaction probabilities and the distinct statistics for free path lengths when leaving a collision versus a deterministic location.

**Nonlocal Interaction** Classical linear transport includes a principle of local interaction [Preisendorfer 1965; Grant and Hunt 1969] that follows from the assumption of independent scattering centers. This guarantees that vector collision rate density and radiance (angular flux) are always proportional. The same proportionality holds for the scalar collision rate density and fluence. Classical Monte Carlo estimators and deterministic approximations for flux and collision rate are therefore equivalent up to a constant factor (the macroscopic cross section  $\Sigma_t$ ).

In GRT, a two-point correlation between collisions includes a memory of the distance  $s$  to the previous collision, which appears in the cross section  $\Sigma_{tc}(s)$  [Larsen 2007; Larsen and Vasques 2011]. This non-Markovian property breaks the local proportionality of collision rate density and flux [d'Eon 2013; De Mulatier et al. 2014]. We find that moment-preserving diffusion approximations, Green's functions and Monte Carlo estimators therefore require distinct forms in GRT, depending upon whether or not the desired physical quantity to estimate is proportional to the collision rate or to the flux.

**Dual Statistics** Multiple scattering in a bounded homogeneous system with spatial correlation exhibits two distinct classes of free-path statistics: those for the free-path lengths between collisions, and those for paths originating at a deterministic location, such as on a boundary [Audic and Frisch 1993]. From these statistics, a pair of distinct attenuation laws for the system immediately follow [d'Eon 2018]. Intuition for the distinction between these statistics is easily found by considering a simple slab of well-separated particles (Figure 1). We use the label 'c' for correlated origins and 'u' for uncorrelated (deterministic) origins and denote the two free-path distributions  $p_c(s)$  and  $p_u(s)$ , with attenuation laws  $X_c(s)$  and  $X_u(s)$  (for further details, which we summarize in Table 1, see [d'Eon 2018]).

To account for dual statistics in GRT, both  $\Sigma_{tc}(s)$  and  $\Sigma_{tu}(s)$  can appear in the new Monte Carlo estimators, depending on the statistical correlation of the previous path vertex to the scatterers. Similarly, two classes of emission lead to distinct source terms:  $Q_c(\mathbf{x})$  for emission from the correlated microstructure, and  $Q_u(\mathbf{x})$  for uncorrelated emission, which produce distinct Green's functions and diffusion approximations depending on the spatial correlation of the point source to the scatterers. In contrast to classical transport, which exhibits effectively only one point source Green's function (up to a constant), in GRT we find four (correlated/uncorrelated, collision-rate/fluence).

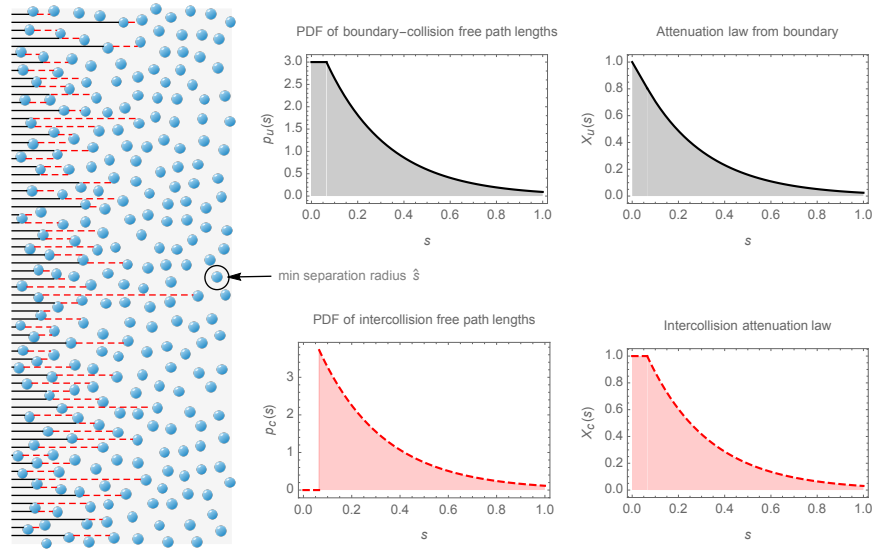


**Figure 1:** When scatterers in a random medium are spatially correlated, the free-path length statistics between collisions are necessarily distinct from those for paths beginning at a boundary interface. Here we illustrate the case of negatively-correlated convex scatterers separated by a minimum distance  $\hat{s} = 0.065$ . For paths beginning at the left boundary of a unit thickness slab (solid-black) collisions can occur arbitrarily close to the boundary and the related path length PDF  $p_u(s)$  and attenuation law  $X_u(s)$  reflect this. Continuing in the same direction from the first collision to the second collision (red-dashed), we find path lengths with a minimum length  $\hat{s}$ . The intercollision free-path distribution  $p_c(s)$  is therefore identically zero for  $s < \hat{s}$  due to the scatterers separation, and the attenuation law between collisions  $X_c(s)$  is 1 for this initial distance.

Symbol	Description	Relations
<i>medium-correlated (stochastic) free path origins</i>		
$s$	distance since last medium collision or correlated birth	
$\Sigma_{tc}(s)$	correlated macroscopic cross section	$\Sigma_{tc}(s) = \frac{p_c(s)}{X_c(s)}$
$p_c(s)$	correlated free-path distribution	$p_c(s) = \Sigma_{tc}(s) e^{-\int_0^s \Sigma_{tc}(s') ds'} = -\frac{\partial}{\partial s} X_c(s) = \langle s_c \rangle \frac{\partial^2}{\partial s^2} X_u(s)$
$X_c(s)$	correlated-origin transmittance	$X_c(s) = 1 - \int_0^s p_c(s') ds'$
$\langle s \rangle_c$	mean correlated free-path	$\langle s \rangle_c = \int_0^\infty p_c(s) s ds$
$\langle s_c^2 \rangle$	mean squared correlated free-path	$\langle s_c^2 \rangle = \int_0^\infty p_c(s) s^2 ds$
<i>medium-uncorrelated (deterministic) free path origins</i>		
$s$	distance since last surface/boundary or uncorrelated birth	
$\Sigma_{tu}(s)$	uncorrelated macroscopic cross section	$\Sigma_{tu}(s) = \frac{p_u(s)}{X_u(s)}$
$p_u(s)$	uncorrelated (equilibrium) free-path distribution	$p_u(s) = \Sigma_{tu}(s) e^{-\int_0^s \Sigma_{tu}(s') ds'} = -\frac{\partial}{\partial s} X_u(s) = \frac{X_c(s)}{\langle s \rangle_c}$
$X_u(s)$	uncorrelated-origin transmittance	$X_u(s) = 1 - \int_0^s p_u(s') ds'$
$\langle s_u \rangle$	mean uncorrelated free-path	$\langle s_u \rangle = \int_0^\infty p_u(s) s ds$

**Table 1:** Summary of our notation and relationships between quantities in GRT.

**Motivation and Approach** The application of infinite medium Green’s functions to solve linear transport problems in bounded domains has seen broad use, especially in tissue optics [Farrell et al. 1992; Kienle and Patterson 1997] and computer graphics [Jensen et al. 2001; Donner and Jensen 2005]. Deterministic solutions to model problems also find use in biased acceleration methods [Fleck and Canfield 1984] or unbiased importance-sampling and guiding of Monte Carlo methods towards zero-variance estimation [Dwivedi 1982; Hoogenboom 2008]. The deterministic methods in this paper are derived with the future goal of extending these approaches to materials where the transport is better represented by the nonexponential random flights of GRT.

From the generalized Peierls’s integral equation for nonexponential random flights [Grosjean 1951; Larsen and Vasques 2011] we derive exact point-source Green’s functions using a Fourier transform approach [Grosjean 1951; Zoia et al. 2011; d’Eon 2013]. For the case of Gamma-2 flights<sup>1</sup> in 3D, we find analytic Green’s functions in the point- and plane-source cases, and these produce the first exact GRT benchmark solutions (which play an important role in linear transport theory [Ganapol 2008]). For most other correlations, however, the Fourier inversion cannot be performed analytically, and the efficiency of the exact solutions is then limited. For these cases, we also derive compact diffusion approximations.

In forming diffusion approximations, there is a degree of arbitrariness based on the desired physical quantities to be preserved [Larsen 2010]. We choose a moment-preserving approach such that the first two even spatial moments of selected scalar quantities are exactly preserved by the approximations. We derive multiple approximations for both the fluence  $\phi(r)$  and the collision rate density  $C(r)$ , considering both uncorrelated and correlated emission. In the case of collision rate density, the mean number of collisions  $\langle r^0 C(r) \rangle$  and mean-square distance of collision  $\langle r^2 C(r) \rangle$  are exactly preserved. For the fluence derivations, the total energy in flight and mean square distance (from the source) of energy in flight are simultaneously preserved by exactly preserving  $\langle r^0 \phi(r) \rangle$  and  $\langle r^2 \phi(r) \rangle$ .

<sup>1</sup> Several works [Frank et al. 2015; Vasques 2016; Makine et al. 2018] have noted that Gamma-2 random flights produce diffusion solutions in 3D. However, by applying a local/classical conversion from collision rate to fluence, which does not hold in GRT, their conclusions about the fluence are approximate.

For each of the four Green’s functions, we derive two diffusion approximations: the classical  $P_1$  diffusion approximation, where all orders of scattering are accounted for by a single diffusion mode, and also a hybrid modified-diffusion approximation due to Grosjean [1956a] that separates out the exact uncollided term and represents the remainder with a diffusion mode. This specific form of modified diffusion was chosen for its increased performance for high absorption levels and near sources, and has proven useful in the classical case when rendering tissue in computer graphics [d’Eon and Irving 2011; d’Eon 2014] and predicting the appearance of 3D-printed materials [Papas et al. 2013].

For piecewise-homogeneous media with general scattering laws, we also generalize the collision and track-length estimators for GRT. Our approach follows Spanier et al. [1969; 1966], beginning with the definition of the analog random walk for GRT in bounded scenes. We then generalize the collision estimators to permit a general class of fictitious scattering that, in the limit of infinite fictitious density, produces the track-length estimators for either collision rates or flux integrals. We find that separate tallies are required for collision rates and fluxes, and that the collision and track-length estimators can be used together during the same random walk to estimate both quantities simultaneously. Nonanalog walks, implicit capture and next-event estimation are also discussed.

## 1.1 Related Work

In this paper<sup>2</sup> we use “GRT” to refer specifically to any linear non-Beerian transport process that discards the notion of exponential free-path distributions (FPDs) characterized only by a mean, and instead forms semi-Markov random flights using the ensemble-averaged two-point intercollision free-path statistics exhibited by a given random medium [Grosjean 1951; Alt 1980; Audic and Frisch 1993; Peltoniemi 1993; Davis 2006; Larsen 2007; Moon et al. 2007; Taine et al. 2010; Larsen and Vasques 2011; Davis and Xu 2014]. We intentionally exclude higher-order memory [Myneni et al. 1991], stochastic absorption and phase functions [Jarabo et al. 2018] and heterogeneous mean densities [Bitterli et al. 2018], all of which would significantly complicate some of the present derivations.

**Motivation for GRT** The primary goal of GRT is to extend linear transport methodology to cover a wider class of participating media while avoiding the significant challenge of exactly solving a fully stochastic equation of radiative transfer [Frisch 1968; Papanicolau and Keller 1971; Ishimaru 1978; Borovoi 2006]. In stochastic radiative transfer, the medium properties become random variables in order to statistically account for unresolved spatial and temporal fluctuations that inevitably arise in any realistic system [Williams 1974]. The desired transport quantities to estimate are then the mean collision rates and fluxes over all possible realizations of the medium. Homogenization to an effective classical medium with exponential attenuation is only accurate when the magnitude of such fluctuations is small and the correlation lengths are on the

---

<sup>2</sup> Our use of “GRT” follows Davis et al. [2014], but we apply it to a broader class of reciprocal transport processes with general intercollision statistics.

order of the wavelength [Ryzhik et al. 1996; Barabanenkov and Finkel’berg 1968; Wen et al. 1990; Tsang et al. 2000]. In many systems, such as dense suspensions of particles [Ishimaru and Kuga 1982; Moon et al. 2007], clumpy molecular clouds [Boissé 1990; Witt and Gordon 1996; Witt and Gordon 2000], terrestrial atmospheres [Davis et al. 1996; Marshak et al. 1997; Pfeilsticker 1999; Kostinski 2001], manufactured materials with random voids [Barthelemy et al. 2008; Svensson et al. 2013; Svensson et al. 2014], hot atomic vapors [Mercadier et al. 2009], shielding materials [Becker et al. 2014] and pebble-bed reactors [Larsen and Vasques 2011], significant deviation from Beer-Lambert attenuation is observed. The impact of such strong correlations on the mean transport can be severe [Torquato 2016].

GRT is an efficient and approximate form of scalar stochastic radiative transfer formed by

- assuming nonstochastic (independent of  $s$ ) single-scattering albedo  $c$  and phase function  $P$
- noting that the mean intercollision free-path statistics  $p_c(s)$  averaged over all realizations of the medium is nonexponential [Audic and Frisch 1993; Moon et al. 2007; Larsen and Vasques 2011]
- adopting a nonexponential random flight that exactly exhibits  $p_c(s)$ , and assuming all higher-order correlation negligible.

GRT is agnostic to how  $p_c(s)$  is determined. It may be estimated using Monte Carlo sampling within specific realizations of quenched disorder [Audic and Frisch 1993; Moon et al. 2007; Larsen and Vasques 2011], by deterministic analysis of a periodic structure [Golse 2012], or from observed statistics of the motion of organic material [Alt 1980; Kareiva and Shigesada 1983]. Alternatively,  $p_c(s)$  follows from specifying any one of  $\Sigma_{rc}(s)$ ,  $\Sigma_{tu}(s)$ ,  $p_u(s)$ ,  $X_c(s)$ ,  $X_u(s)$ , by relationships summarized in Table 1. The mean attenuation law from a deterministic origin  $X_u(s)$  may be measured in the laboratory, or calculated from a given stationary random function for  $\Sigma_t$  [Levermore et al. 1988; Williams 1997; Kostinski 2001; Davis and Mineev-Weinstein 2011; Larsen and Clark 2014; Frankel et al. 2017; Banko et al. 2019; Guo et al. 2019].

**Reciprocity** The need for dual statistics in bounded domains was first noted by Audic and Frisch [1993], who estimated  $p_c(s)$  using Monte Carlo. In the first part of this work [d’Eon 2018], we showed that Helmholtz reciprocity for a diffuse law of reflection in a GRT half space requires the relationship

$$p_c(s) = \langle s_c \rangle \frac{\partial^2}{\partial s^2} X_u(s) \quad (1)$$

where  $\langle s_c \rangle$  is a constant—the mean-free-path length between collisions<sup>3</sup>. This greatly simplifies the specification of media in GRT, bypassing the need for Monte Carlo free-path histograms in [Audic and Frisch 1993]. Bitterli et al. [2018] subsequently confirmed Equation 1 in an alternative derivation based on mean attenuation laws in continuous random media, noting that  $X_u(s)$  is the mean attenuation over all realiza-

<sup>3</sup> For Lévy walks with unbounded mean free paths [Liemert and Kienle 2017; Binzoni et al. 2018], truncation to a finite mean [Mantegna and Stanley 1994] is required.

tions, and  $X_c(s)$  is the mean attenuation over only those realizations with a scatterer at the start ( $s = 0$ ).

Dual free-path length statistics have also appeared in several other studies. It was observed in the periodic Lorentz gas [Golse 2012] and is also the reason why the Milne problem in a binary mixture has two definitions/solutions [Pomraning 1989]. The relationship in Equation 1 corresponds to known relationships between chord lengths and lineal path functions in heterogeneous materials [Torquato and Lu 1993], and was first suggested in a bounded random flight [Mazzolo 2009] in order to preserve a remarkable invariance property of chord lengths in convex uniformly-illuminated random media, first proven for exponential media [Bardsley and Dubi 1981; Blanco and Fournier 2003] and then extended to nonexponential free paths [Mazzolo 2009; Mazzolo et al. 2014], and more recently observed in the laboratory [Savo et al. 2017].

Without accounting for this distinction in GRT, several related works speak only of “the attenuation law” and produce nonreciprocal transport in bounded domains [Davis 2006; Taine et al. 2010; Davis and Xu 2014; Wrenninge et al. 2017]. However, the methods in this paper also apply for these formalisms.

**Monte Carlo Methods for Nonclassical Transport** Fictitious scattering in non-classical transport has been previously proposed as an acceleration scheme of the chord-length sampling algorithm in the context of multiphase multidimensional mixtures [Ambos and Mikhailov 2011]. This differs from our use of fictitious scattering to transition from collision to track-length estimation in the context of completely general free-path statistics.

The classical track-length estimator has also been previously applied for estimating fluence in non-classical transport [Boissé 1990; Liemert and Kienle 2017], but not generalized to estimate collision rates.

Bitterli et al. [2018] generalized Veach’s path-integral formulation of light transport for GRT, manipulating terms to produce a fully reciprocal model suitable to bidirectional estimators. This formulation is complementary to our present investigations of reaction rate and fluence estimates using track-length estimators.

**Relationship to Stochastic Processes Literature** The Monte Carlo and deterministic methods in this paper apply generally to any stochastic processes where a particle moves along straight paths at constant speed between collisions that change the particle’s direction and possibly absorb the particle. This includes some, but not all, of the stochastic processes that are studied under names such as Lévy walks [Uchaikin and Gusarov 1997; Zaburdaev et al. 2015], random evolutions [Hersh 1974], velocity jump process [Othmer and Hillen 2000] and semi-Markov random flights [Grosjean 1951; Dutka 1985; Majumdar and Ziff 2008; Zoia et al. 2011; Le Caër 2011; De Gregorio 2012; De Gregorio and Orsingher 2012; Pogorui and Rodríguez-Dagnino 2013; De Gregorio 2017].

**The Generalized Linear Boltzmann Equation** In classical linear transport, various equivalent mathematical approaches are loosely divided into two camps [Guth and In-

önü 1960; Wigner 1992] based on whether or not the focus is on the history of a single particle (random flight) or on a single volume element (Boltzmann). The nonexponential random flights of GRT have been studied since the early 1900s [Grosjean 1951; Dutka 1985]. The related generalized linear Boltzmann equation (GLBE) for GRT was more recently proposed and the connection to the integral equation of random flight established [Larsen 2007; Larsen and Vasques 2011]. Existence and uniqueness of solutions for the GLBE have been established [Frank et al. 2010] and the GLBE has been extended to support anisotropic random correlated media [Vasques and Larsen 2014] with direction-dependent cross sections. Other Boltzmann-like equations have appeared [Peltoniemi 1993; Golse 2012; Rukolaine 2016; Binzoni et al. 2018], and some equivalences between them have been established [Larsen et al. 2017]. The most relevant aspect of these works to the present is not the integro-differential form of the transport equation, however, but the formalism of total macroscopic cross sections  $\Sigma_t(s)$  with a free-path-length memory variable  $s$ . Through this lens, nonexponential random flights take on a familiar linear-transport character, and the subtleties of collision rate and flux balance and generalization of familiar Monte Carlo methods become more evident.

**Diffusion Asymptotics for Nonclassical Transport** The Green’s function derivations and related moment-preserving diffusion approximations in this paper expand upon our previous work [d’Eon 2013] by including the case of uncorrelated emission, and by performing a completely general moment analysis in the Fourier domain that avoids the previous need for Fourier inversions. In addition to proving conjectures from this previous work, we also prove new results about the diffusion coefficient’s dependence on spatial dimension  $d$ . The relationship to other diffusion asymptotics derived from a parameter-of-smallness approach [Frank et al. 2010; Larsen and Vasques 2011] is also discussed.

We do not presently consider diffusion approximations that preserve the rigorous “asymptotic” diffusion length  $\kappa_{tr}$ , which may be desired in deep-penetration and shielding applications. For expanded approximations in classical transport that preserve both multiple even spatial moments and  $\kappa_{tr}$  see [Grosjean 1963b; Grosjean 1963a] and [Larsen 2010]. For a  $\kappa_{tr}$ -preserving diffusion approximation of collision rate density under correlated emission in GRT, see [d’Eon 2013]. Also, alternatives to diffusion, such as saddlepoint methods [Gatto 2017], may be preferred in some cases, but are not treated presently.

**Relationship to Wave Scattering Theories** Theories for wave propagation in random media are closely related to the scalar equations of radiative transfer (RT) that neglect polarization and interference aspects [Keller 1962; Ishimaru 1991; Apresyan and Kravtsov 1996]. Originally criticized for being phenomenological, more recently RT has enjoyed a strengthened relationship to “honest” wave formalisms [Mishchenko 2008], a relationship that continues to evolve and surprise [Pierrat et al. 2014]. Wave theories for stochastic media have considered the influence of correlation and have proposed analogous concepts to those in scalar GRT. The recognition of the non-Markovian property of wave transport in spatially-correlated random media and the

suggestion of two-point memory as a practical simplification goes back at least as far as Hoffman ([1964], p.137). Also, in the discrete picture of a random medium, the observation of the nonlocal relationship between total and exciting fields is similar to the nonlocal proportionality of collision rate density and fluence in GRT; “what relation exists between the exciting field acting on a scatterer at a point, and the total field which would exist at that point if the scatterer were not there” [Waterman and Truell 1961]. The early theories of Foldy and Lax assumed a constant proportionality, but correlation exists in any realistic medium and the exact relationship between the exciting and total fields is that of an operator ([Frisch 1968] p.172).

## 1.2 Outline

The paper is structured into three main theoretical sections and concludes with a discussion. In Section 2 we examine the nonlocal proportionality between collision rate and flux that motivates the following theory. In Section 3, we generalize the collision and track-length estimators for GRT. In Section 4, we derive the infinite medium Green’s functions for isotropic point sources with isotropic scattering in a monoenergetic steady-state setting. The Green’s functions and Monte Carlo estimators are used to cross validate each other in Section 4.3. Related moment-preserving diffusion approximations are derived in Section 5. A number of related (but untested) details relating to Monte Carlo estimation in GRT are included in Appendix B.

## 2 The Balance of Flux and Collision Rate

To motivate the following sections, we begin by recalling the relationship between collision rate and flux in both classical and generalized time-independent linear transport theories. We denote the *collision rate density*<sup>4</sup>  $C(\mathbf{x}, \vec{\omega})$ , where

$$C(\mathbf{x}, \vec{\omega})dVd\vec{\omega} = \text{rate at which particles in } dVd\vec{\omega} \quad (2)$$

about  $(\mathbf{x}, \vec{\omega})$  enter collisions

and denote its scalar counterpart, the *scalar collision rate density*

$$C(\mathbf{x}) = \int_{4\pi} C(\mathbf{x}, \vec{\omega})d\vec{\omega}. \quad (3)$$

We denote the *scalar flux* (fluence rate)  $\phi(\mathbf{x})$ , which is the angular integral of the *vector-flux* (radiance)  $\psi(\mathbf{x}, \vec{\omega})$ ,

$$\phi(\mathbf{x}) = \int_{4\pi} \psi(\mathbf{x}, \vec{\omega})d\vec{\omega}. \quad (4)$$

### 2.1 Classical Local Balance

Classical linear transport theory assumes that a particle at position  $\mathbf{x}$  traveling in direction  $\vec{\omega}$  traversing an incremental distance  $ds$  has an incremental collision probability

<sup>4</sup> [Liemert and Kienle 2017] use “radiance” for vector collision rate density, which risks causing confusion with respect to the density of particles in flight.

$dp$  given by

$$dp = \Sigma_t(\mathbf{x}, \vec{\omega})ds, \quad (5)$$

which directly implies Beer-Lambert attenuation. The *transmittance*

$$X(\mathbf{x}, s, \vec{\omega}) = e^{-\int_0^s \Sigma_t(\mathbf{x}+t\vec{\omega})dt} \quad (6)$$

is the dimensionless probability of flying uncollided along a straight path between  $\mathbf{x}$  and  $\mathbf{x} + s\vec{\omega}$  and is an exponential of the optical distance. A closely related quantity is the distribution of free-path lengths  $p(\mathbf{x}, s, \vec{\omega})$ , a probability density function (PDF) with units  $m^{-1}$ .

A *free path* is the joint occurrence of two things: first flying uncollided along a path of length  $s$  with probability  $X(\mathbf{x}, s, \vec{\omega})$ , and then entering a collision in the next incremental path distance  $ds$ ,

$$p(\mathbf{x}, s, \vec{\omega})ds = X(\mathbf{x}, s, \vec{\omega})\Sigma_t(\mathbf{x} + s\vec{\omega})ds. \quad (7)$$

In classical transport, the two components of the free path are independent: the collision process has no memory of how far the particle has flown. This allows the inverse mean free path  $\Sigma_t$  to locally convert between collision rates and fluxes. If the integral of the scalar flux  $\phi(\mathbf{x})$  in some region  $V$  is known and if  $\Sigma_t(\mathbf{x})$  can be assumed constant in  $V$ , then the collision rate in  $V$  can be found directly by multiplication by  $\Sigma_t(\mathbf{x})$ ,

$$\int_V C(\mathbf{x})dV = \Sigma_t(\mathbf{x}) \int_V \phi(\mathbf{x})dV. \quad (8)$$

Conversely, if  $\Sigma_t(\mathbf{x}) > 0$  then the flux integral can be found from the collision rate by division by  $\Sigma_t(\mathbf{x})$ . This transformational power of  $\Sigma_t$  is used in many other classical scenarios. Monte Carlo methods estimating both reaction rates and flux integrals can use a single tally structure that subdivides phase space and decide after the simulation what quantities to derive from it. Classical Green's functions and diffusion equations for flux are also convertible to those for collision rate by multiplication by  $\Sigma_t$ .

## 2.2 Local Imbalance in GRT

In GRT, the balance of collision rate and flux is nonlocal due to the short-term memory. The cross sections are extended to depend on  $s$  [Larsen and Vasques 2011], which gives an incremental collision probability following a collision of

$$dp = \Sigma_{tc}(\mathbf{x}, \vec{\omega}, s)ds \quad (9)$$

and

$$dp = \Sigma_{tu}(\mathbf{x}, \vec{\omega}, s)ds \quad (10)$$

if the previous scene interaction was a deterministic location, such as a boundary surface. This non-local collision probability breaks the classical balance of flux and collision rate<sup>5</sup>.

Consider negatively correlated scattering centers in the context of Figure 2, where  $\Sigma_{tc}(\mathbf{x}, \vec{\omega}, s)$  is low or possibly zero for small  $s$  to prevent short distances between collisions. Having arrived at  $V$ , the two particles have different collision probabilities within

<sup>5</sup> Note also that this same issue arises for the scalar quantities in anisotropic random media due to the dependence of  $\Sigma_t(\vec{\omega})$  on direction.

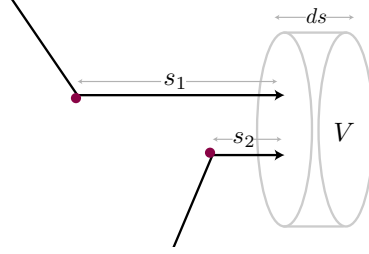


**Figure 2:** When the scatterers in a homogeneous random medium are spatially correlated, the probability of a collision includes a memory term. The macroscopic cross section  $\Sigma_{tc}(s)$  depends on  $s$ , the distance since previous collision, and the probability of collision when traversing a path of incremental distance  $ds$  is  $\Sigma_{tc}(s)ds$ . The collision rate in  $V$  is estimated by the traditional collision estimator, scoring the particle weight  $W$  for each collision in the region. However, a track-length estimator for the collision rate in  $V$  must score  $W \int_s^{s+ds} \Sigma_{tc}(s')ds'$  to account for the collision probability changing with free-path length  $s$ . Conversely, for estimating the flux integral in  $V$ , the traditional track length estimator, scoring  $W$ -weighted track-lengths in  $V$ , maintains its familiar form, but the collision estimator must be modified to score  $W/\Sigma_{tc}(s)$ . If both flux integral and collision rate are desired in  $V$ , two distinct tallies must be kept.

$V$ . Particle 2 may have less chance to collide in  $V$  than particle 1, or even see zero collision probability, because of the proximity of its previous collision to  $V$ . The ratio of total track-lengths passing through  $V$  to the total number of collisions created within  $V$  will depend on the distribution of free-path lengths  $s$  before crossing  $V$  and, thus, on the state of the system outside of  $V$ . Therefore, to estimate both flux-proportional and collision-rate-proportional reaction rates from a single tally in GRT would require tallying over  $s$  and using

$$\int_V C(\mathbf{x})dV = \int_V \int_0^\infty \Sigma_t(\mathbf{x}, s)\phi(\mathbf{x}, s)dsdV, \quad (11)$$

where  $\phi(\mathbf{x}, s)$  is the spectral decomposition of the scalar flux over path-length parameter  $s$ ,

$$\phi(\mathbf{x}, s) = \int_{4\pi} \psi(\mathbf{x}, \vec{\omega}, s)d\vec{\omega}. \quad (12)$$

The  $s$ -spectral flux  $\psi(\mathbf{x}, \vec{\omega}, s)$  decomposes the traditional angular flux over  $s$  and is required to form a local integro-differential form of the transfer equation, requiring an extra integration over  $s$  [Larsen and Vasques 2011] and is related to the scalar flux by

$$\phi(\mathbf{x}) = \int_0^\infty \phi(\mathbf{x}, s)ds. \quad (13)$$

Given, amongst other things, the goal of global fluence tallies in reactor design [Martin 2012], we would prefer to avoid increasing the dimensionality of tally structures. We achieve this by generalizing Monte Carlo estimators for estimating both quantities, and by keeping separate tallies.

### 3 Monte Carlo Estimators in GRT

In this section we propose generalizations of collision and track-length estimators for time-independent monoenergetic linear transport problems in GRT. We assume a phase space  $\Gamma$  with positions  $\mathbf{x}$  and unit directions  $\vec{\omega}$  in Euclidean  $\mathbb{R}^d$  space,  $\mathcal{P} = (\mathbf{x}, \vec{\omega}) \in \Gamma$ .

#### 3.1 Collision-Rate-Proportional Estimation

We first consider estimation of quantities  $I$  that are linear functionals of the collision-rate density by specifying a measurement or “detector” function  $g(\mathcal{P})$ ,

$$I = \int_{\Gamma} g(\mathcal{P})C(\mathcal{P})d\mathcal{P}. \quad (14)$$

Monte Carlo estimators for  $I$  are derived from the integral equation for  $C$ ,

$$C(\mathbf{x}, \vec{\omega}) = \int_0^{s_b[\mathbf{x}, -\vec{\omega}]} \int_{4\pi} K(\mathbf{x} - s\vec{\omega}, \vec{\omega}' \rightarrow \mathbf{x}, \vec{\omega})C(\mathbf{x} - s\vec{\omega}, \vec{\omega}')d\vec{\omega}' ds + S_0(\mathbf{x}, \vec{\omega}) + S_B(\mathbf{x}, \vec{\omega}) \quad (15)$$

where  $s_b[\mathbf{x}, \vec{\omega}]$  is a ray-tracing function that returns the distance  $s_b$  from  $\mathbf{x}$  along  $\vec{\omega}$  to the nearest boundary. The intercollision transport kernel  $K$  combines the fraction of particles scattered, their change in direction and their next free path,

$$K(\mathbf{x}', \vec{\omega}' \rightarrow \mathbf{x}, \vec{\omega}) = cP(\vec{\omega}' \rightarrow \vec{\omega}; \mathbf{x}')p_c(\|\mathbf{x} - \mathbf{x}'\|). \quad (16)$$

To support reciprocal GRT, we have modified (15) from the previous form [Larsen and Vasques 2011] in two ways. The density of initial collisions

$$S_0(\mathbf{x}, \vec{\omega})dVd\vec{\omega} =$$

the rate at which particles scatter into  $dVd\vec{\omega}$

about  $(\mathbf{x}, \vec{\omega})$  directly from sources  $Q$

includes contributions from the new uncorrelated-origin source  $Q_u$ ,

$$S_0(\mathbf{x}, \vec{\omega}) = \int_0^{s_b[\mathbf{x}, -\vec{\omega}]} (Q_c(\mathbf{x} - s\vec{\omega}, \vec{\omega})p_c(s) + Q_u(\mathbf{x} - s\vec{\omega}, \vec{\omega})p_u(s)) ds. \quad (17)$$

Here,  $Q_u$  accounts for both sources at the boundary and internal sources emitting from medium-uncorrelated locations. We also include an optional term  $S_B$  that accounts for the first collisions that follow surface reflection and transmission events for problems with reflecting and refracting boundary conditions. This requires knowing the angular flux leaving the boundary location  $\mathbf{x} - s_b[\mathbf{x}, -\vec{\omega}]\vec{\omega}$  which is found by tracing along  $-\vec{\omega}$  from  $\mathbf{x}$ .

$$S_B(\mathbf{x}, \vec{\omega}) = \psi(\mathbf{x} - s_b[\mathbf{x}, -\vec{\omega}]\vec{\omega}, \vec{\omega})p_u(s_b) \quad (18)$$

The angular flux  $\psi(\mathbf{x}_b, \vec{\omega})$  leaving a boundary surface location  $\mathbf{x}_b$  in direction  $\vec{\omega}$  is found by integrating the angular flux arriving there  $\psi_i(\mathbf{x}_b, \vec{\omega}')$  with the bidirectional surface reflection distribution function (BSDF) [Pharr et al. 2016]  $f_s(\mathbf{x}_b, \vec{\omega}, \vec{\omega}')$ , which accounts for reflectance and transmittance,

$$\psi(\mathbf{x}_b, \vec{\omega}) = \int_{4\pi} f_s(\mathbf{x}_b, \vec{\omega}, \vec{\omega}')\psi_i(\mathbf{x}_b, \vec{\omega}')|\vec{n} \cdot \vec{\omega}'|d\vec{\omega}', \quad (19)$$

where  $\vec{n}$  is the surface normal. The angular flux arriving at the surface *from* direction  $-\vec{\omega}$  is

$$\psi_i(\mathbf{x}_b, -\vec{\omega}) = \psi(\mathbf{x}_b - \vec{\omega}s_b[\mathbf{x}_b, -\vec{\omega}], \vec{\omega})X_u(s_b[\mathbf{x}_b, -\vec{\omega}]) + \int_0^{s_b[\mathbf{x}_b, -\vec{\omega}]} \int_{4\pi} C(\mathbf{x} - s\vec{\omega}, \vec{\omega}')cP(\vec{\omega}' \rightarrow \vec{\omega})X_c(s)d\vec{\omega}' ds, \quad (20)$$

the sum of the flux scattered into  $-\vec{\omega}$  from collisions in the volume together with the uncorrelated transmittance of flux leaving the first surface found in that direction.

### 3.2 The Analog Walk for GRT

To build estimators for  $I$ , we begin with the analog walk for GRT, which is very similar to the classical case. A random walk  $w = (\mathbf{x}_0, \vec{\omega}_0), \dots, (\mathbf{x}_k, \vec{\omega}_k)$  begins by source sampling  $(\mathbf{x}_0, \vec{\omega}_0, E)$  from the union of the sources,  $Q_c$  and  $Q_u$ , in direct proportion to their relative powers. The initial vertex  $(\mathbf{x}_0, \vec{\omega}_0)$  of  $w$  is this sampled source location and direction. The initial free-path length  $s_0$  is sampled from either  $p_c(s)$  (in the case  $Q_c$  was sampled) or  $p_u(s)$  (otherwise). Additional vertices are added by repeating the following process. Subsequent positions are determined via

$$\mathbf{x}_{i+1} = \mathbf{x}_i + \min(s_i, s_b[\mathbf{x}_i, \vec{\omega}_i]) \vec{\omega}_i. \quad (21)$$

Now, currently at position  $\mathbf{x}_{i+1}$ , either the phase function at the current volume interior point or analog<sup>6</sup> sampling of the BSDF at the current boundary surface determine the next direction  $\vec{\omega}_{i+1}$ . If escape or absorption is sampled, the walk terminates. Otherwise, a medium collision is followed with a new free-path length  $s_{i+1}$  sampled from  $p_c(s)$  and a surface interaction is followed with a sample from  $p_u(s; \mathbf{x}_{i+1})$  for the current volume region (which may have changed).

### 3.3 The Collision Estimator

Nothing about the inclusion of two sources, non-exponential free-path statistics or boundary reflections materially alters the proof [Spanier and Gelbard 1969] that, for the analog random walk  $w$ ,

$$\sum_{i=1}^{k(w)} g(\mathbf{x}_i, \vec{\omega}_i) \quad (22)$$

is an unbiased estimator for  $I$ . With  $g(\mathbf{x}, \vec{\omega}) = 1$  for all interior points of some region  $V$  of the medium and 0 elsewhere, Eq.(22) is an unbiased estimate of the collision rate  $\int_V C(\mathbf{x})dV$ , in  $V$ . By definition of the analog walk, collisions are created in the same proportion to the physical process they model, and so this is expected. Note that, in our notation, vertices of  $w$  corresponding to boundary surface interactions avoid contributing to the collision rate or measurement  $I$  by defining  $g$  to be 0 exactly at the boundary.

<sup>6</sup> Analog sampling of BSDFs is uncommon in practice for surfaces that absorb energy. To be precise, an analog sampling process for a BSDF returns weight 0 (an absorption event) with a probability of  $1 - \alpha(\vec{\omega}_i)$  where  $\alpha(\vec{\omega}_i)$  is the albedo of the material for the current incoming direction  $\vec{\omega}_i$ , and returns direction  $\vec{\omega}$  (with weight 1) in proportion to  $|\vec{n} \cdot \vec{\omega}|f_s(\vec{\omega}, \vec{\omega}_i)$  otherwise.

### 3.3.1 Estimating Flux with the Collision Estimator

In classical linear transport, estimating flux using the collision estimator makes use of the classical balance of flux and collision rate. For each collision, by Eq.(5), there is, on average, a free-path of length  $1/\Sigma_t$  required to make that collision possible. Thus,  $g$  is set to  $g(\mathbf{x}, \vec{\omega}) = 1/\Sigma_t(\mathbf{x}, \vec{\omega})$  in  $V$ . This limits the measurement of flux to regions where collisions occur ( $\Sigma_t(\mathbf{x}) > 0$ ). Where no collisions occur, alternative deterministic calculations can often be applied [Case et al. 1953]. As  $\Sigma_t$  decreases, the performance of the collision estimator degrades, making the track-length estimator indispensable in optically-thin regions.

In GRT, flux estimation with the collision estimator can have additional limitations. We see immediately from Eq.(9) that the free-path lengths crossing  $\mathbf{x}$  required to create the known collision rate there depend on  $s$ , requiring a collision estimator with

$$g^*(\mathbf{x}, \vec{\omega}, s) = \begin{cases} \frac{1}{\Sigma_{tc}(\mathbf{x}, \vec{\omega}, s)} & \text{for collisions with correlated origins} \\ \frac{1}{\Sigma_{tu}(\mathbf{x}, \vec{\omega}, s)} & \text{otherwise.} \end{cases} \quad (23)$$

Eq.(23) with Eq.(22) is an unbiased estimator for the flux, under certain restrictions, but we see that flux estimation in GRT is no longer a linear functional of the collision rate with a local kernel  $g(\mathbf{x}, \vec{\omega})$ . We have labeled this estimation with a star because  $s$  is not in the phase space and therefore Eq.(23) is incompatible with Eq.(14). Ultimately, we define the class of flux-proportional measurements  $I_\psi$  to be linear functionals of the spectral collision-rate density,

$$I_\psi = \int_{\Gamma^*} g^*(\mathcal{P}^*) C(\mathcal{P}^*) d\mathcal{P}^* \quad (24)$$

where we have extended the phase space  $\mathcal{P}^* = (\mathbf{x}, \vec{\omega}, s) \in \Gamma^*$  to include free-path parameter  $s$ . The *spectral collision-rate density* is

$$C(\mathbf{x}, \vec{\omega}, s) dV d\vec{\omega} ds \quad (25)$$

= rate at which particles in  $dV d\vec{\omega} ds$   
about  $(\mathbf{x}, \vec{\omega}, s)$  enter collisions

providing a decomposition of the collision density over the distance  $s$  since previous scene interaction. The analog random walk previously defined can also be used to estimate measurements of class  $I_\psi$  because the path-length  $s$  is known at each step in the walk generation, so Eq.(23) with Eq.(22) is a practical estimator in some cases.

Similar to the classical case, the performance of Eq.(23) will be limited by the lowest value of  $\Sigma_{tc}(s)$  over  $s$ . Note that this is no longer a local limitation applying only to optically thin regions, but to the entire piecewise homogeneous volume element. Furthermore, if there exists a range of finite width  $0 < a < s < b$  with  $\Sigma_{tc}(s)$  identically zero on this range while also  $\Sigma_{tc}(s) > 0$  for some portion of  $s > b$ , then the free path distribution has a gap where no collisions ever occur, but where flux arises from traversing that gap and colliding later with non-zero probability. If so, then this collision estimator is incompatible with flux estimation *everywhere*.

*Example 1:* Consider negatively correlated scattering centers in a 3D slab with uniform plane-parallel illumination arriving normally on one side (Figure 1). Figure 3 illustrates

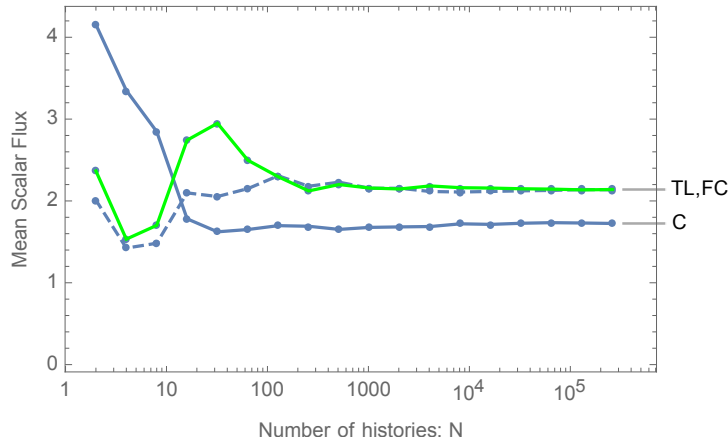


**Figure 3:** Comparison of Monte Carlo estimation of the total scalar flux in a purely-scattering 3D slab with negatively-correlated scatterers. The classical collision estimator (C) underestimates the flux because the macroscopic cross-section (Equation 26) has an optically-empty gap between collisions. A modified collision estimator with fictitious scattering (FC, dashed) or a track-length estimator (TL, green) is required to accurately estimate the flux.

the inability of the collision estimator  $1/\Sigma_{tc}(s)$  to estimate flux inside a unit thickness slab with intercollision macroscopic cross-section

$$\Sigma_{tc}(s) = \begin{cases} 0 & s < \hat{s} \\ \frac{1}{\ell - \hat{s}} & \text{else} \end{cases} \quad (26)$$

due to the optically empty gap  $0 < s < \hat{s}$ . In this example, we consider conservative ( $c = 1$ ) isotropic scattering, with  $\ell = 0.333$  and minimum intercollision free-path lengths of  $\hat{s} = 0.065$ .

### 3.3.2 Fictitious Scattering

Some of the limitations of the collision estimator for flux in GRT can be mitigated by introducing fictitious matter along the free-path sampling portion of the walk such that collision with the fictitious matter ultimately causes the particle to scatter forward with no loss, as if the matter wasn't there. This applies the Woodcock/delta-tracking method used for heterogeneous volumes, but in a homogeneous setting, analogous to the class of estimators introduced by Spanier [Spanier 1966; Lux 1978a; Lux 1978b]. Increased density of collision in “optically thin” portions of the free path lower the variance of the estimator in those regions. The trade-off is additional cost of computation time to perform the walk.

Intuition for this generalization is found from conceptualizing correlated random media as a classical heterogeneous medium that changes each time a collision occurs due to

its short term memory. The last sampled collision in the medium collapses the set of all possible random realizations down to only those where such a scattering event could have occurred, applying  $\Sigma_{tc}(r)$  radially around the point of the last known collision. Using Woodcock/delta tracking to form random walks within this collapsed medium in the presence of additional fictitious density, keeping the real density field  $\Sigma_{tc}(r)$  fixed until a real collision is sampled, extends the collision estimator and, in the limit of infinite fictitious density everywhere, yields the track-length estimators for GRT. In the case of an uncorrelated free path, such as entry at a boundary, the medium is initialized to equilibrium with all possible random realizations in equal probability. As this path extends into the medium, the memory of finding no collisions up to distance  $s$  continuously collapses the nature of the medium via  $\Sigma_{tu}(s)$  (which is why  $\Sigma_{tu}(s)$  is not a constant) until a collision occurs and then the medium snaps to  $\Sigma_{tc}(r)$ .

The collision estimator for GRT is extended with fictitious scattering by choosing  $\Sigma^*(s)$  such that  $\Sigma^*(s) \geq \Sigma_{t-}(s)$  for all  $s > 0$ . Both correlated- and uncorrelated-origin free paths may independently perform the generalizations in this section, choosing the same or different  $\Sigma^*(s)$ . We describe simply  $\Sigma_{t-}(s)$  for this derivation to mean either.

Having chosen  $\Sigma^*$ , free path lengths for the walk  $w$  are modified to sample from

$$p^*(s) = \Sigma^*(s) e^{-\int_0^s \Sigma^*(s') ds'}. \quad (27)$$

At each medium collision of the walk, the collision type (real vs fictitious) is decided randomly with probability  $p_\delta$  for fictitious collisions

$$p_\delta(s) = \frac{\Sigma^*(s) - \Sigma_{t-}(s)}{\Sigma^*(s)}. \quad (28)$$

Both real and fictitious collisions add vertices to the walk  $w$ . Source sampling and boundary collisions are treated identically to the standard case. Real collisions determine  $\vec{\omega}_{i+1}$  from the phase function with probability  $c$ , resetting  $s$  to 0, and terminate the walk with absorption otherwise. Fictitious collisions continue walking along  $\vec{\omega}_{i+1} = \vec{\omega}_i$  with probability 1 but  $s$  is *not reset* to 0—a critically important difference for applying this method to GRT. This requires sampling tails of  $p^*(s)$ . If the current distance to the previous real collision is  $s_r$ , then we must sample the next free-path length  $s$  from,

$$p(s) = \frac{p^*(s + s_r)}{\int_{s_r}^{\infty} p^*(s') ds'}. \quad (29)$$

If  $\Sigma^*$  is a constant that bounds  $\Sigma_{t-}(s)$  everywhere, then the tails are exponential and all free-path lengths can be sampled using  $s = -\frac{1}{\Sigma^*} \log \xi$ , where  $\xi \in (0, 1)$  is a uniform random number. However, a majorant of  $\Sigma_{t-}(s)$  might not exist or use of one might not be desired (due to inefficiency), requiring a more general  $\Sigma^*(s)$ . We discuss tail sampling further in Section B.5.

Collisions now occur  $1/(1 - p_\delta(s))$  more frequently than in the analog walk. To form an unbiased estimator, the fictitious collision estimator must weight the scores at each collision vertex by the inverse of this proportionality,

$$\sum_{i=1}^{k(w)} g^*(\mathbf{x}_i, \vec{\omega}_i) (1 - p_\delta(s_{i-1})) = \sum_{i=1}^{k(w)} g^*(\mathbf{x}_i, \vec{\omega}_i) \frac{\Sigma_{t-}(s)}{\Sigma^*(s)}. \quad (30)$$

This estimator can fill empty or low portions of the correlated free-path distribution to permit flux estimation in scenarios where it would otherwise fail or perform poorly. In the limit that  $\Sigma^*(s) \rightarrow \infty$  for all  $s$ , we form estimators of the track-length type that score continuously along segments of the walk.

*Example 1 (continued):* Returning to Example 1, defined above, we form a new collision estimator that fills the optically-empty portion of the intercollision free paths with fictitious matter using  $\Sigma^* = 1/(\ell - \hat{s})$ , leaving the collision estimator for the uncorrelated entry step unchanged ( $1/\Sigma_{tu}(s)$ ). Figure 3 shows the new collision estimator converging to the exact solution, which we verify using a track-length estimator, described next. For  $N = 10^8$  histories, the fictitious collision estimator estimated a mean of 2.1658 in 34.4s with a variance of 5.07. The track-length estimator estimated a mean of 2.1340 in 27.4s with a variance of 4.36.

### 3.4 The Track-length Estimator for GRT

Taking the limit in Eq.(30) that, for all  $s > 0$ ,  $\Sigma^*(s) \rightarrow \infty$ , following the same arguments as the classical derivation [Spanier 1966], we find the track-length estimator for GRT,

$$\sum_{i=0}^{k(w)-1} \int_0^{||x_{i+1}-x_i||} g^*(\mathbf{x}_i + s\vec{\omega}_i, \vec{\omega}_i, s) \Sigma_{t_{-(i)}}(s) ds. \quad (31)$$

Here, the notation  $\Sigma_{t_{-(i)}}$  means

$$\Sigma_{t_{-(i)}} = \begin{cases} \Sigma_{tc} & \text{if } \mathbf{x}_i \text{ is a medium-correlated origin} \\ \Sigma_{tu} & \text{if } \mathbf{x}_i \text{ is a medium-uncorrelated origin.} \end{cases} \quad (32)$$

#### 3.4.1 The Track-length Estimator for Flux

Noting that the collision estimator in Eq.(23) for flux in some region  $V$  scores the inverse of the path-length dependent macroscopic cross-section in that region and 0 elsewhere, we see that this term cancels in the track-length estimator. Hence, the track-length estimator reduces to scoring the total length of all tracks passing through  $V$ , and so is, in some sense, *the* track-length estimator in that it scores the length of the track (as opposed to scoring along it). Just as it was no surprise that the collision estimator for collision rate required no change in GRT, here too we expect this result, especially in light of the International Commission on Radiation Units and Measurements definition of fluence [Lux and Koblinger 1991].

#### 3.4.2 The Track-length Estimator for Collision Rate

Noting that the collision estimator for collision rate in some region  $V$  scores 1 in that region and 0 elsewhere, we see that the track-length estimator in GRT for collision rate scores,

$$\int_{s_1}^{s_2} \Sigma_{t_{-}}(s) ds, \quad (33)$$

the integral of  $\Sigma_{t_{-}}(s)$  for any portion of a track that lies within  $V$ , where  $\{s_1, s_2\}$  indexes that track subsegment. In some scenarios, such as when the free-path distribution has

been determined by the histogram sampling approach [Audic and Frisch 1993; Moon et al. 2007; Larsen and Vasques 2011], this estimator would be the least attractive of the four, in needing to compute unique integrals per score. These integrals may have no simple closed form or may be inconvenient to derive from a discrete histogram. However, for many parametric analytic correlated forms of transport, this limitation is not much of a concern.

Later in the paper we consider two specific non-exponential free-path distributions. The Gamma-2 distribution  $p_c(s) = e^{-s}s$  has  $\Sigma_{tc}(s) = \frac{s}{1+s}$  and therefore scores

$$\int_{s_1}^{s_2} \Sigma_{tc}(s) ds = s_2 - s_1 - \log\left(\frac{1+s_2}{1+s_1}\right) \quad (34)$$

for correlated-origin tracks and

$$\int_{s_1}^{s_2} \Sigma_{tu}(s) ds = s_2 - s_1 - \log\left(\frac{2+s_2}{2+s_1}\right). \quad (35)$$

for uncorrelated-origin tracks.

We also consider a power-law attenuation law [Davis and Xu 2014], adopting the reciprocal imbedding proposed in [d'Eon 2018; Jarabo et al. 2018]. The correlated free path distribution is then

$$p_c(s) = a(a+1)\ell(al)^a(al+s)^{-a-2} \quad (36)$$

with correlated mean free path length  $\langle s_c \rangle = \ell$  and shape parameter  $a > 1$ . Exponential attenuation is recovered in the limit  $a \rightarrow \infty$ . The track-length integrals for power-law transport are

$$\int_{s_1}^{s_2} \Sigma_{tc}(s) ds = (a+1) \log\left(\frac{al+s_2}{al+s_1}\right) \quad (37)$$

$$\int_{s_1}^{s_2} \Sigma_{tu}(s) ds = a \log\left(\frac{al+s_2}{al+s_1}\right) \quad (38)$$

This power-law free-path distribution was derived from a continuum model of stochastic density with Gamma-distributed noise of parameter  $a$  [Davis and Mineev-Weinstein 2011]. Using the inverse Laplace transform of  $p_c(s)$  (with  $\langle s_c \rangle = \ell = 1$ ) we find that this free-path distribution is a Gamma-distributed superposition of positive exponential free-path distributions,

$$p_c(s) = \int_0^\infty \frac{a^a e^{-a\Sigma_t} \Sigma_t^a}{\Gamma(a)} \Sigma_t e^{-\Sigma_t s} d\Sigma_t. \quad (39)$$

One interpretation of this is that a free path in this family of correlated random media with mean cross-section  $\hat{\Sigma}_t = 1$  is equivalent to choosing a random classical cross-section  $\Sigma_t > 0$  from the normalized gamma distribution

$$\frac{a^a e^{-a\Sigma_t} \Sigma_t^a}{\Gamma(a)} \quad (40)$$

and keeping this cross section fixed until the next collision.

To test the new Monte Carlo estimators, we derive benchmark solutions for infinite homogeneous media in the next section. Additional discussion of implicit capture,

zero-variance guiding and the duality of two classes of estimators is included in Appendix B.

## 4 Green's Functions for the Isotropic Point Source

We now turn to the derivation of exact solutions for the monoenergetic time-independent scalar collision rate density  $C(\mathbf{x})$  and scalar flux  $\phi(\mathbf{x})$  about an isotropically-emitting point source in an infinite isotropically-scattering medium. In the case of emission that is spatially correlated to the scattering centers in the medium, we reproduce the derivations of a previous work [d'Eon 2013] for the *correlated collision rate Green's function*  $C_c(\mathbf{x})$  and *correlated scalar flux Green's function*  $\phi_c(\mathbf{x})$ . Two new solutions,  $C_u(\mathbf{x})$  and  $\phi_u(\mathbf{x})$ , for the case of uncorrelated emission, are derived to form a complete set of infinite medium Green's functions for reciprocal generalized linear transport.

Consider a unit power isotropic point source at the origin of the infinite homogeneous medium with single-scattering albedo  $0 < c < 1$  and isotropic scattering. The scalar collision-rate density  $C(\mathbf{x})$  at position  $\mathbf{x} \in \mathbb{R}^d$  is the solution of the generalized Peierls integral equation [Grosjean 1951; Larsen and Vasques 2011]

$$C(\mathbf{x}) = C_0(\mathbf{x}) + c \int_{\mathbb{R}^d} C(\mathbf{x}') \frac{p_c(\|\mathbf{x} - \mathbf{x}'\|)}{\Omega_d(\|\mathbf{x} - \mathbf{x}'\|)} d\mathbf{x}', \quad (41)$$

where the surface area of the sphere of radius  $r$  in  $\mathbb{R}^d$  is written

$$\Omega_d(r) = \frac{d\pi^{d/2} r^{d-1}}{\Gamma(\frac{d}{2} + 1)}, \quad (42)$$

and  $C_0(\mathbf{x})$  is the collision rate density of first collisions in the system arising directly from two isotropically-emitting sources,

$$C_0(\mathbf{x}) = \int_{\mathbb{R}^d} Q_c(\mathbf{x}') \frac{p_c(\|\mathbf{x} - \mathbf{x}'\|)}{\Omega_d(\|\mathbf{x} - \mathbf{x}'\|)} d\mathbf{x}' + \int_{\mathbb{R}^d} Q_u(\mathbf{x}') \frac{p_u(\|\mathbf{x} - \mathbf{x}'\|)}{\Omega_d(\|\mathbf{x} - \mathbf{x}'\|)} d\mathbf{x}'. \quad (43)$$

For the case of a single point source, exactly one of  $Q_c(\mathbf{x})$  and  $Q_u(\mathbf{x})$  is a Dirac delta  $\delta(\mathbf{x})$  at the origin and the other is 0.

Equation 41 differs from the case of classical radiative transfer by permitting arbitrary free-path length statistics between collisions via  $p_c(s)$ , and reduces to the familiar form when all free-path length statistics are exponential,  $p_c(s) = p_u(s) = \Sigma_t \exp[-s \Sigma_t]$  (the unique scenario where  $Q_c$  and  $Q_u$  become equivalent). As in the classical case, the primary challenge is solving for  $C(\mathbf{x})$ . Once  $C(\mathbf{x})$  is known, the scalar flux  $\phi(\mathbf{x})$  follows directly from spatial integration with a transmittance kernel, described below.

A Neumann series solution of Equation 41 can be formed by repeated convolution of uncollided propagators, interleaved with absorption. We employ a Fourier transform approach [Grosjean 1951; Zoia et al. 2011], where the required convolutions are easily formed. The radial symmetry of the emission produces solutions depending on a single spatial coordinate  $r$ , the distance from the point source, so this problem is typically termed a 1D transport problem, but it describes a symmetric transport process in  $\mathbb{R}^d$ .

We will make use of the following forward and inverse spherical Fourier transforms of a radially-symmetric function  $f(r)$  (with radius  $r \geq 0$ ) in  $\mathbb{R}^d$  [Dutka 1985]

$$\bar{f}(z) = \mathcal{F}_d\{f(r)\} = z^{1-d/2}(2\pi)^{d/2} \int_0^\infty r^{d/2} J_{d/2-1}(rz) f(r) dr \quad (44)$$

$$f(r) = \mathcal{F}_d^{-1}\{\bar{f}(z)\} = \frac{r^{1-d/2}}{(2\pi)^{d/2}} \int_0^\infty z^{d/2} J_{d/2-1}(rz) \bar{f}(z) dz \quad (45)$$

where  $z$  is the transformed coordinate relating to  $r$  and  $J_k$  is the modified Bessel function of the first kind.

#### 4.1 Collision Rate Density

We now introduce the *correlated-origin propagator*

$$\zeta_c(r) = \frac{p_c(r)}{\Omega_d(r)} \quad (46)$$

and the *uncorrelated-origin propagator*

$$\zeta_u(r) = \frac{p_u(r)}{\Omega_d(r)} \quad (47)$$

where the probability of finding a particle entering a collision within  $dr$  of distance  $r$  from its previous medium event is  $\zeta_c(r)dr$  if the previous event was a medium collision or birth from a source correlated in location to the scatterers, and  $\zeta_u(r)dr$  otherwise. These distributions describe only spatial translations between collision events and are energy-conserving,

$$\int_0^\infty \Omega_d(r) \zeta_c(r) dr = \int_0^\infty \Omega_d(r) \zeta_u(r) dr = 1. \quad (48)$$

Absorption is assumed to occur at the scattering centers and the single-scattering albedo  $c$  is assumed independent of the track length  $s$  between collisions.

Combining the propagators and  $c$ , the Neumann series solution of Equation 41 is readily formed as a geometric series of convolutions. For example, the density of particles entering their second collision after correlated birth is given by the absorption-weighted convolution  $c \zeta_c(r) \star \zeta_c(r)$ , the third collision density by  $c^2 \zeta_c(r) \star \zeta_c(r) \star \zeta_c(r)$ , and so on. We denote the Fourier transforms of the propagators

$$\mathcal{F}_d\{\zeta_c(r)\} = \bar{\zeta}_c(z), \quad (49)$$

$$\mathcal{F}_d\{\zeta_u(r)\} = \bar{\zeta}_u(z) \quad (50)$$

and solve for the various Green's functions in the frequency domain. Exact or numerical Fourier inversion is used in numerical application of these results, which we discuss at the end of this section.

##### 4.1.1 Correlated Emission (Collision rate)

In the frequency domain, the initial distribution of collisions for correlated emission is given directly by  $\bar{\zeta}_c(z)$ , with subsequent collision orders found by repeated application

of the kernel  $c \bar{\zeta}_c(z)$  that includes both absorption and further propagation. Thus, the total collision rate density including all orders of scattering is

$$C_c(r) = \mathcal{F}_d^{-1} \left\{ \frac{\bar{\zeta}_c(z)}{1 - c \bar{\zeta}_c(z)} \right\}. \quad (51)$$

Separating out the initial collision density from the multiply-collided portion yields,

$$C_c(r) = \frac{p_c(r)}{\Omega_d(r)} + \mathcal{F}_d^{-1} \left\{ \frac{c (\bar{\zeta}_c(z))^2}{1 - c \bar{\zeta}_c(z)} \right\}, \quad (52)$$

which is recommended when numerically inverting the Fourier solution, and also used later for the derivation of non-classical diffusion approximations.

#### 4.1.2 Uncorrelated Emission (Collision rate)

In the case of uncorrelated emission, the initial propagation is given by  $\zeta_u(r)$ , and all subsequent propagations are given by the kernel  $c \bar{\zeta}_c(z)$ , so the uncorrelated Green's functions for collision rate density are related to the correlated case by a factor of  $\frac{\bar{\zeta}_u(z)}{\bar{\zeta}_c(z)}$ , giving

$$C_u(r) = \mathcal{F}_d^{-1} \left\{ \frac{\bar{\zeta}_u(z)}{1 - c \bar{\zeta}_c(z)} \right\} \quad (53)$$

and

$$C_u(r) = \frac{p_u(r)}{\Omega_d(r)} + \mathcal{F}_d^{-1} \left\{ \frac{c \bar{\zeta}_c(z) \bar{\zeta}_u(z)}{1 - c \bar{\zeta}_c(z)} \right\}. \quad (54)$$

## 4.2 Scalar Flux / Fluence

The scalar flux about the isotropic point source is given by the sum of the uncollided flux leaving the collisions and the uncollided flux leaving the point source directly. A frequency domain construction requires use of the *stretched transmittance for correlated emission*

$$\chi_c(r) = \frac{X_c(r)}{\Omega_d(r)}, \quad (55)$$

a related distribution for uncorrelated emission

$$\chi_u(r) = \frac{X_u(r)}{\Omega_d(r)} \quad (56)$$

and their Fourier transforms,

$$\mathcal{F}_d\{\chi_c(r)\} = \bar{\chi}_c(z), \quad (57)$$

$$\mathcal{F}_d\{\chi_u(r)\} = \bar{\chi}_u(z). \quad (58)$$

#### 4.2.1 Correlated Emission (Flux)

In the case of correlated emission, the uncollided flux directly from the point source is given by  $\chi_c(r)$  and the flux from the collisions is  $\bar{\chi}_c(z) c \bar{C}_c(z)$  giving a total of

$$\phi_c(r) = \mathcal{F}_d^{-1} \left\{ \bar{\chi}_c(z) + \bar{\chi}_c(z) c \frac{\bar{\zeta}_c(z)}{1 - c \bar{\zeta}_c(z)} \right\} = \mathcal{F}_d^{-1} \left\{ \frac{\bar{\chi}_c(z)}{1 - c \bar{\zeta}_c(z)} \right\} \quad (59)$$

or, keeping the uncollided flux separate,

$$\phi_c(r) = \frac{X_c(r)}{\Omega_d(r)} + \mathcal{F}_d^{-1} \left\{ \frac{c \bar{\chi}_c(z) \bar{\zeta}_c(z)}{1 - c \bar{\zeta}_c(z)} \right\}. \quad (60)$$

Given the proportionality between uncorrelated free-path distribution and attenuation, we also have that the Green's functions  $C_u(r)$  and  $\phi_c(r)$  are proportional

$$\phi_c(r) = \langle s_c \rangle C_u(r). \quad (61)$$

#### 4.2.2 Uncorrelated Emission (Flux)

For the case of uncorrelated emission, the uncollided flux directly from the point source is given by  $\chi_u(r)$  and the flux from the collisions is  $\bar{\chi}_c(z) c \bar{C}_u(z)$  giving a total of

$$\phi_u(r) = \mathcal{F}_d^{-1} \left\{ \bar{\chi}_u(z) + \bar{\chi}_c(z) c \frac{\bar{\zeta}_u(z)}{1 - c \bar{\zeta}_c(z)} \right\} \quad (62)$$

or

$$\phi_u(r) = \frac{X_u(r)}{\Omega_d(r)} + \mathcal{F}_d^{-1} \left\{ \frac{c \bar{\chi}_c(z) \bar{\zeta}_u(z)}{1 - c \bar{\zeta}_c(z)} \right\}. \quad (63)$$

### 4.3 Numerical Validation

We compared analytic and semi-analytic numerical predictions of the Green's functions derived in this section to Monte Carlo estimations of the corresponding collision rate and flux quantities and noted no difference apart from Monte Carlo noise. A variety of absorption levels ( $c \in \{0.01, 0.1, 0.3, 0.5, 0.7, 0.8, 0.9, 0.95, 0.99\}$ ) were tested for transport in three dimensions with a correlated free-path distribution given by

$$p_c(s) = e^{-s} s \quad (64)$$

with intercollision mean free path  $\langle s_c \rangle = 2$ . For both collision rate and flux integral quantities, we tested collision estimators for the point source problem and tested track-length estimators for an equivalent plane-source problem. Our findings are briefly summarized below. For additional validation of Eqs. (51) or (52) for the case of correlated emission with other free-path distributions and general spatial dimensions ( $d \in \{2, 3, 4\}$ ) see d'Eon [2013].

### 4.3.1 Point-Source Validation

The Gamma free-path distribution in Eq. 64 leads to uncorrelated free-paths [d'Eon 2018]

$$p_u(s) = \frac{1}{2}e^{-s}(1+s) \quad (65)$$

and macroscopic cross-sections given by

$$\Sigma_{rc}(s) = \frac{s}{1+s}, \quad (66)$$

$$\Sigma_{uu}(s) = \frac{1+s}{2+s}. \quad (67)$$

The free propagators in the frequency domain, found by combining Eqs 64 and 65 with Eqs 49, are

$$\bar{\zeta}_c(z) = \frac{1}{1+z^2}, \quad (68)$$

$$\bar{\zeta}_u(z) = \frac{1}{2} \left( \frac{1}{1+z^2} + \frac{\tan^{-1}(z)}{z} \right). \quad (69)$$

From Eq. 51, the correlated collision rate density in the frequency domain is

$$\bar{C}_c(z) = \frac{1}{1-c+z^2}, \quad (70)$$

which inverts into the scalar diffusion point-source Green's function for the 3D medium,

$$C_c(r) = \mathcal{F}_3^{-1} \left\{ \frac{1}{1-c+z^2} \right\} = \frac{e^{-r\sqrt{1-c}}}{4\pi r}. \quad (71)$$

For the case of collision rate due to uncorrelated emission, using Eq. 54, we find<sup>7</sup>

$$C_u(r) = \frac{e^{-r}(1+r)}{8\pi r^2} + \frac{c}{4\pi^2 r} \int_0^\infty \frac{\left( \frac{z}{1+z^2} + \tan^{-1}(z) \right)}{(1-c+z^2)} \sin(rz) dz, \quad (72)$$

which we compare in Figure 4 to Monte Carlo estimation using the analog collision estimator.

For the stretched transmittances, we find (Eqs. 55 and 56)

$$\bar{\chi}_c(z) = \frac{1}{z^2+1} + \frac{\tan^{-1}(z)}{z}, \quad (73)$$

$$\bar{\chi}_u(z) = \frac{1}{2z^2+2} + \frac{\tan^{-1}(z)}{z}, \quad (74)$$

producing the scalar flux Green's function about a correlated point source,

$$\phi_c(r) = 2C_u(r) \quad (75)$$

<sup>7</sup> This integral can be solved by solving an equivalent problem in plane geometry and using the plane to point transform. See Appendix A.

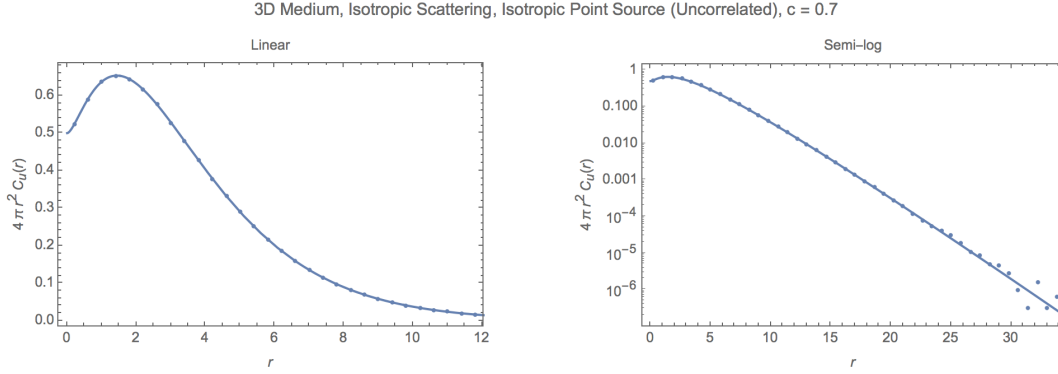


**Figure 4:** Collision estimation of collision rate density  $C_u(x)$  at a distance  $r$  from an isotropic uncorrelated point source in infinite 3D media with isotropic scattering and correlated free-path distribution  $p_c(s) = se^{-s}$ . Monte Carlo (dots) vs analytic (continuous, Equation 72).

and the scalar flux Green's function about an uncorrelated point source,

$$\phi_u(r) = \frac{X_u(r)}{4\pi r^2} + \mathcal{F}_3^{-1} \left\{ \frac{c \left( (z^2 + 1) \tan^{-1}(z) + z \right)^2}{2z^2 (z^2 + 1) (-c + z^2 + 1)} \right\} \quad (76)$$

$$= \frac{e^{-r}(2+r)}{8\pi r^2} + \int_0^\infty \frac{c \left( z + (1+z^2) \tan^{-1}(z) \right)^2 \sin(rz)}{4\pi^2 r z (1+z^2) (1-c+z^2)} dz. \quad (77)$$

In Figure 5 we show several examples of the cross validation of Eqs. (75) and (76) with Monte Carlo estimation using a generalized collision estimator for the flux integrals where at each collision the flux score is  $(1+s)/s$ , except for the first collision following uncorrelated emission, which scores  $(2+s)/(1+s)$ .

#### 4.3.2 Plane-Source Validation

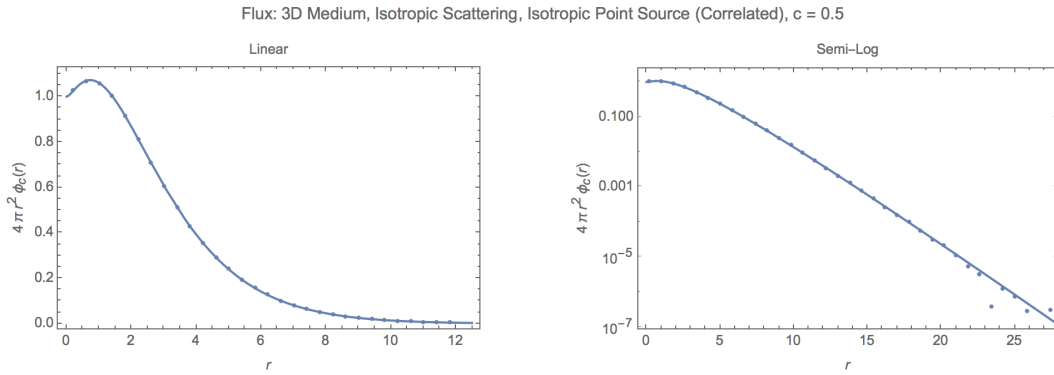
Given the simpler track-length calculation with a finite slab versus a finite shell, we chose to test the track-length estimators in Section 3 about an isotropic plane source in infinite 3D media. Applying the point-to-plane transform [Case et al. 1953]

$$\phi_{\text{pl}}(x) = 2\pi \int_{|x|}^\infty \phi_{\text{pt}}(r) r dr, \quad (78)$$

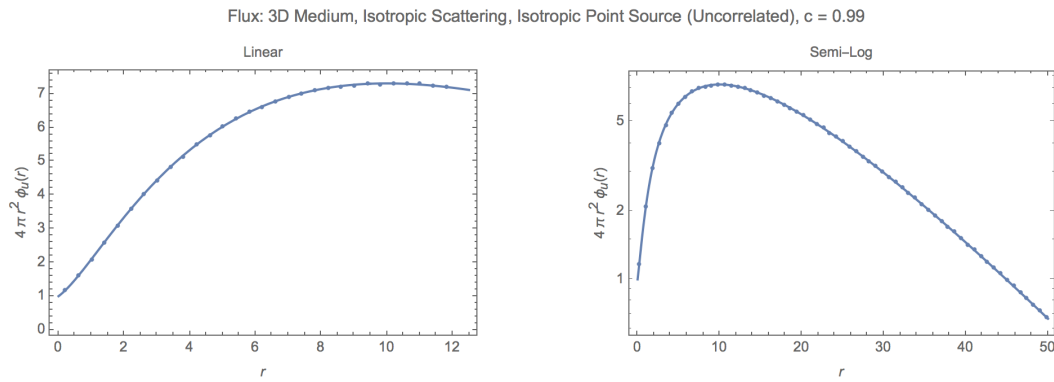
to the Fourier inversion for 3D space (Eq. 44 with  $d = 3$ ) we find that any given Fourier-space distribution  $\bar{g}(z)$  has a primal space inversion about an isotropic plane source given by

$$g(x) = \frac{1}{\pi} \int_0^\infty \bar{g}(z) \cos(xz) dz = \frac{1}{\pi} \int_{-\infty}^\infty g(z) e^{-izx} dz \quad (79)$$

which is simply the Fourier inversion of the even function  $\bar{g}(z)$ . It happens that in any dimension  $d$  Eq. 79 converts the spherical-geometry Green's functions derived in this section to the related Green's function for an isotropically-emitting hyper-plane source.



(a) Correlated emission (Equation 75)



(b) Uncorrelated emission (Equation 76)

**Figure 5:** Flux about an isotropic point source in a 3D medium. Monte Carlo collision estimator (dots) vs analytic (continuous).

Selecting  $\bar{g}(z)$  to be the scalar flux for the correlated point source in Eq. 75 and using Eq. 79 we find the scalar flux about the isotropic plane source to be

$$\phi_c(x) = \frac{e^{-|x|} + E_1(|x|)}{2} + \frac{1}{\pi} \int_0^\infty \frac{c(z + (1+z^2)\tan^{-1}(z)) \cos(xz)}{z(1+z^2)(1-c+z^2)} dz \quad (80)$$

where  $E_1$  is the exponential integral function  $E_1(z) = \int_1^\infty e^{-zt}/t dt$ . A similar calculation for the case of uncorrelated emission yields

$$\phi_u(x) = \frac{1}{4} \left( e^{-|x|} + 2E_1(|x|) \right) + \frac{1}{\pi} \int_0^\infty \frac{\left( c(z + (1+z^2)\tan^{-1}(z))^2 \right) \cos(xz)}{2z^2(1+z^2)(1-c+z^2)} dz. \quad (81)$$

To validate these derivations, we performed track-length estimation of the flux integrals at various depths  $z$  about the isotropic plane source, scoring track-lengths within each tally slab of thickness  $dz = 0.2$ . Several comparisons of these deterministic and Monte Carlo results are shown in Figure 6.

For completeness, we also estimated collision densities about the plane sources for both the correlated and uncorrelated emission cases using the new track-length estimators derived in Section 3.4 and validated the results using the Green's function derivations (Figure 7). As in the point-source case, we find a simple diffusion solution for the correlated emission case,

$$C_c(x) = \frac{1}{\pi} \int_0^\infty \frac{1}{1-c+z^2} \cos(xz) dz = \frac{e^{-\sqrt{1-c}|x|}}{2\sqrt{1-c}}, \quad (82)$$

and the uncorrelated collision rate density is proportional to the correlated flux

$$C_u(x) = \frac{1}{2} \phi_c(x). \quad (83)$$

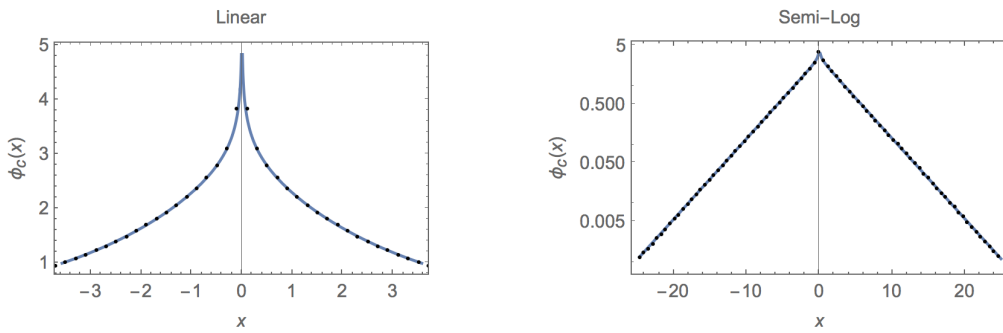
For each free-path segment of the analog random walk, with  $s_1$  and  $s_2$  the range of intersection with a given flux tally volume element (satisfying  $0 \leq s_1 \leq s_2 \leq s$ ), intercollision and correlated birth segments score the integrals previously given in Section 3.4.2.

#### 4.4 Flux / Collision-Rate Balance in Gamma-2 Infinite Media

We briefly consider the ratio of collisions to particles in flight at various distances from the infinite isotropic plane source in the case of correlated emission, comparing the ratio to the classical proportionality  $\langle s_c \rangle C_c(x) / \phi_c(x) = 1$ . Figure 8 (a) illustrates that, for a variety of absorption levels, we see sub-classical collision rates near the plane source and super-classical collision rates as  $x \rightarrow \infty$ , with the classical balance occurring at a location that is increasingly far from the plane source as  $c \rightarrow 1$ . In the limit of increasing distance from the source we find that the ratio tends to a non-classical proportionality unless the scattering is conservative ( $c = 1$ ),

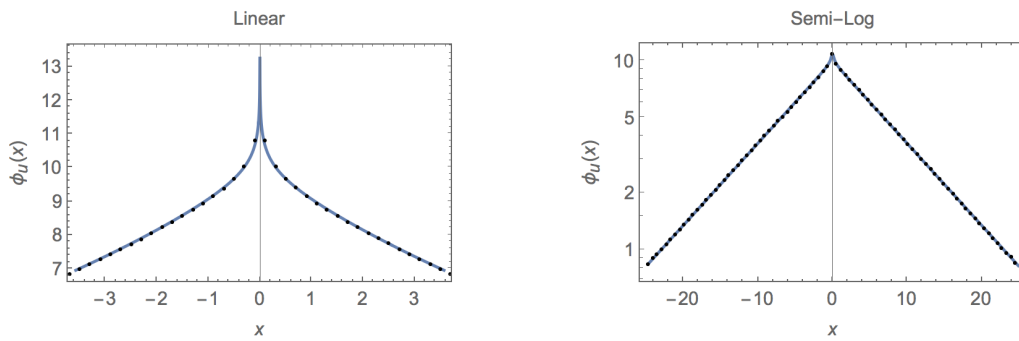
$$\lim_{x \rightarrow \infty} \frac{\langle s_c \rangle C_c(x)}{\phi_c(x)} = \frac{2}{1 + \frac{c \tanh^{-1}(\sqrt{1-c})}{\sqrt{1-c}}}. \quad (84)$$

3D Medium, Isotropic Scattering, Isotropic Plane Source (Correlated),  $c = 0.9$   
 Scalar Flux  $\phi_c(x)$



(a) Correlated emission (Equation 80)

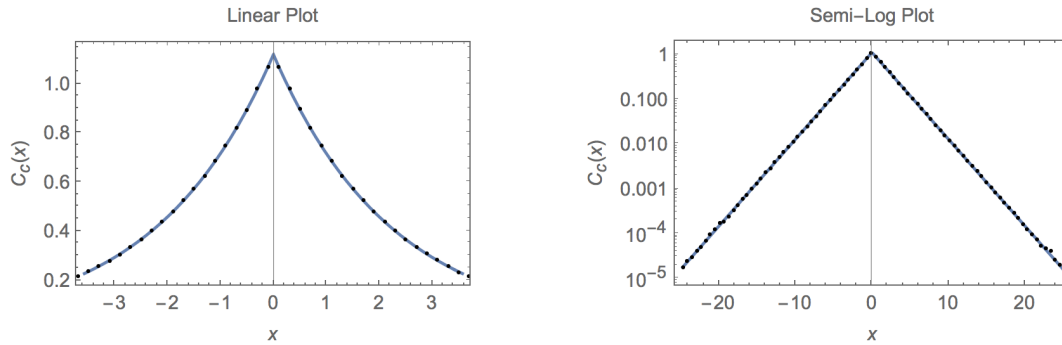
3D Medium, Isotropic Scattering, Isotropic Plane Source (Uncorrelated),  $c = 0.99$   
 Scalar Flux  $\phi_u(x)$



(b) Uncorrelated emission (Equation 81)

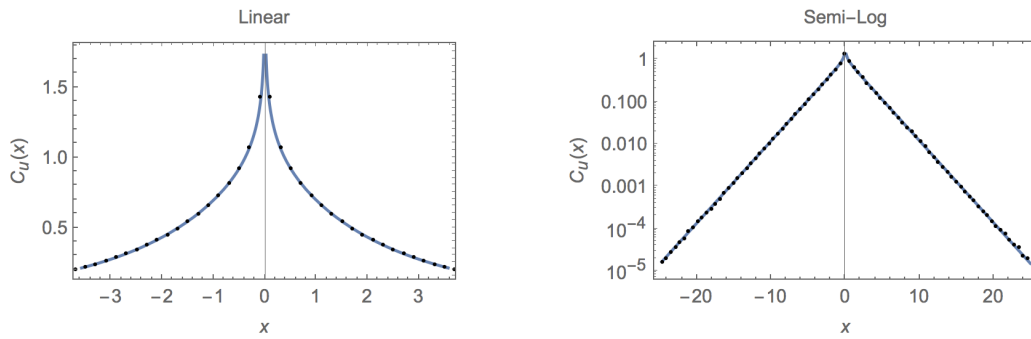
**Figure 6:** Scalar flux density  $\phi(z)$  at positions  $z$  from an isotropic plane source in infinite 3D media. Track-length Monte Carlo collision estimation (dots) vs analytic (continuous).

3D Medium, Isotropic Scattering, Isotropic Plane Source (Correlated),  $c = 0.8$   
Collision Rate Density  $C_c(x)$



(a) Correlated emission (Equation 82)

3D Medium, Isotropic Scattering, Isotropic Plane Source (Uncorrelated),  $c = 0.8$   
Collision Rate Density  $C_u(x)$



(b) Uncorrelated emission (Equation 83)

**Figure 7:** Generalized track-length estimation of collision rate density at a distance  $x$  from an isotropic plane source in infinite 3D media with isotropic scattering and correlated free-path distribution  $p_c(s) = se^{-s}$ . Monte Carlo (dots) vs analytic (continuous).

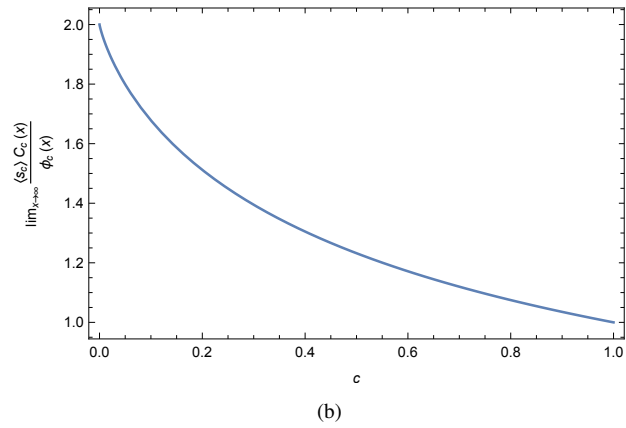
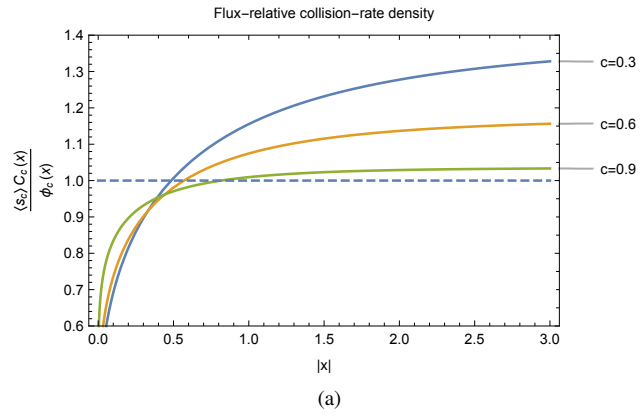


**Figure 8:** For the correlated-emission isotropic plane source in infinite 3D media with correlated free-path distribution  $p_c(s) = e^{-s}s$  and single-scattering albedo  $c$  we show (a) The flux-relative collision rate at distance  $x$  from the source and (b) the limiting behaviour of the ratio at increasing distance from the source as a function of absorption (Equation 84).

The ‘‘rigorous’’ asymptotic diffusion approximation for the correlated scalar flux is thus,

$$\phi_c(x) \approx \frac{(\sqrt{1-c} + c \tanh^{-1}(\sqrt{1-c}))}{2(1-c)} e^{-\sqrt{1-c}|x|} \quad (85)$$

## 5 Diffusion Approximations for GRT

### 5.1 Free-path and transmittance moments

Our diffusion approximations will require the first five spatial moments of the correlated-origin free path distribution  $p_c(s)$ , defined by

$$\langle s_c^m \rangle = \int_0^\infty p_c(s) s^m ds \quad (86)$$

with  $m \in \{1, 2, 3, 4\}$ . The  $m = 0$  moment is unity by normalization of the distribution  $p_c(s)$ . We will also require the 0th and 2nd spatial moments of  $p_u(s)$ ,  $X_c(s)$  and  $X_u(s)$ , which can all be expressed in terms of the first five moments of  $p_c(s)$  using the identity [Vasques and Slaybaugh 2016]

$$\langle s^m \rangle = m \int_0^\infty s^{m-1} X(s) ds \quad (87)$$

where the uncorrelated moments are related to  $s_c$  moments by  $p_u(s) = X_c(s)/\langle s_c \rangle$ . Combining these, we find the moments for correlated transmittance,

$$X_{c0} = \int_0^\infty X_c(s) ds = \langle s_c \rangle \quad (88)$$

$$X_{c2} = \int_0^\infty X_c(s) s^2 ds = \frac{\langle s_c^3 \rangle}{3}, \quad (89)$$

the mean-square uncorrelated free-path

$$\langle s_u^2 \rangle = \int_0^\infty p_u(s) s^2 ds = \frac{\langle s_c^3 \rangle}{3\langle s_c \rangle} \quad (90)$$

and the moments for uncorrelated transmittance,

$$X_{u0} = \int_0^\infty X_u(s) ds = \frac{\langle s_c^2 \rangle}{2\langle s_c \rangle} \quad (91)$$

$$X_{u2} = \int_0^\infty X_u(s) s^2 ds = \frac{\langle s_c^4 \rangle}{12\langle s_c \rangle}. \quad (92)$$

For a given scalar transport quantity  $g(r)$  about an isotropic point source in infinite media, a moment-preserving diffusion approximation can be readily derived provided the moments

$$\langle r^0 g(r) \rangle = \int_0^\infty \Omega_d(r) r^0 g(r) dr \quad (93)$$

and

$$\langle r^2 g(r) \rangle = \int_0^\infty \Omega_d(r) r^2 g(r) dr \quad (94)$$

are known. These moments are related to derivatives of the Fourier-transformed quantity  $\bar{g}(z)$  at  $z = 0$ , as shown in Appendix A of [Zoia et al. 2011], by

$$\langle r^m g(r) \rangle = \frac{\sqrt{\pi} \Gamma\left(\frac{d+m}{2}\right)}{\Gamma\left(\frac{d}{2}\right) \Gamma\left(\frac{1+m}{2}\right)} \frac{\partial^m}{\partial (iz)^m} [\bar{g}(z)]_{z=0} \quad (95)$$

for even  $m \geq 0$  and  $\langle r^m g(r) \rangle = 0$  for odd  $m$ . We only require this result for  $m = 0$ ,

$$\langle r^0 g(r) \rangle = \bar{g}(0) \quad (96)$$

and  $m = 2$ ,

$$\langle r^2 g(r) \rangle = -d \bar{g}''(0). \quad (97)$$

## 5.2 Spherical Diffusion Mode in $d$ Dimensions

The classical steady-state diffusion equation, typically written

$$-D \nabla^2 \phi(\mathbf{x}) + \Sigma_a \phi(\mathbf{x}) = Q(\mathbf{x}) \quad (98)$$

with diffusion constant  $D > 0$  and constant  $\Sigma_a > 0$  has simple solutions in infinite homogeneous media for the isotropic point source  $Q(\mathbf{x}) = \delta(\mathbf{x})$ . The point-source diffusion mode in spatial dimension  $d$  with diffusion length  $\nu = \sqrt{D/\Sigma_a} > 0$  is the inverse spherical Fourier transform

$$m_d(\nu, r) = \mathcal{F}_d^{-1} \left\{ \frac{1}{1 + (z\nu)^2} \right\} = (2\pi)^{-d/2} r^{1-\frac{d}{2}} \nu^{-\frac{d}{2}-1} K_{\frac{d-2}{2}} \left( \frac{r}{\nu} \right) \quad (99)$$

where  $K_n(x)$  is the modified Bessel function of the second kind. The radial diffusion mode for the one-dimensional rod ( $d = 1$ ) is

$$m_1(\nu, r) = \frac{e^{-\frac{r}{\nu}}}{2\nu}, \quad (100)$$

for Flatland ( $d = 2$ ) is

$$m_2(\nu, r) = \frac{K_0\left(\frac{r}{\nu}\right)}{2\pi\nu^2}, \quad (101)$$

and for three dimensions is

$$m_3(\nu, r) = \frac{e^{-\frac{r}{\nu}}}{4\pi r \nu^2}. \quad (102)$$

We chose this form for its unit normalization,

$$\int_0^\infty \Omega_d(r) m_d(\nu, r) = 1, \quad (103)$$

yielding a second spatial moment of

$$\int_0^\infty r^2 \Omega_d(r) m_d(\nu, r) = 2d\nu^2. \quad (104)$$

Our diffusion approximations of a given radially-symmetric scalar quantity  $g(r)$  with moments  $\langle r^0 g(r) \rangle$  and  $\langle r^2 g(r) \rangle$  will be determined directly by approximating the quantity by a diffusion mode with two unknowns  $a$  and  $\nu$ ,

$$g(r) \approx a m_d(\nu, r) \quad (105)$$

and solving for  $a$  and  $v$  given the moments and Eqs.(103) and (104), giving

$$g(r) \approx \langle r^0 g(r) \rangle m_d \left( \sqrt{\frac{\langle r^2 g(r) \rangle}{2d \langle r^0 g(r) \rangle}}, r \right). \quad (106)$$

Much of the complexity of the approximation is in finding the moments, which we solve generally in the remainder of this section. These moment relations should also allow other forms of approximation using two-parameter families of radially-symmetric functions distinct from the diffusion mode. Extending the following derivations to include higher-order moments is straightforward. In the future we hope to investigate the utility of powers of diffusion in frequency space with power  $p \geq 1/2$ , which have simple inversions in all dimensions [Jakeman and Pusey 1976]

$$\mathcal{F}_d^{-1} \left\{ \left( \frac{1}{1 + (zv)^2} \right)^p \right\} = \frac{\pi^{-d/2} 2^{-\frac{d}{2}-p+1} v^{-\frac{d}{2}-p} r^{p-\frac{d}{2}} K_{\frac{1}{2}(d-2p)} \left( \frac{r}{v} \right)}{\Gamma(p)} \quad (107)$$

and permit more general fitting of exact transport solutions in either spherical or planar geometries.

### 5.3 Collision Rate Density

The zeroth moment of the collision rate density  $\langle r^0 C(r) \rangle$  is a uniform integration of collision rate density over all space, which must then equal the mean number of collisions experienced by a single particle given an absorption probability of  $1 - c$  at each collision [Ivanov 1994]

$$\langle r^0 C_c(r) \rangle = \langle r^0 C_u(r) \rangle = \frac{1}{1 - c}, \quad (108)$$

a quantity that is independent of the phase function, free-path distribution(s), spatial dimension or angular distribution of emission. Given its independence on free-path distribution, this quantity is the same for correlated and uncorrelated emission.

#### 5.3.1 Correlated emission

For the classical approach of approximating the entire collision rate density with a single diffusion mode, we require  $\langle r^2 C_c(r) \rangle$  which, by Eqs. 51 and 97, is

$$\langle r^2 C_c(r) \rangle = -d \frac{\partial^2}{\partial z^2} \left[ \frac{\bar{\zeta}_c(z)}{1 - c\bar{\zeta}_c(z)} \right]_{z=0} = \frac{d \left( (1 - c\bar{\zeta}_c(0))\bar{\zeta}_c''(0) + 2c\bar{\zeta}_c'(0)^2 \right)}{(c\bar{\zeta}_c(0) - 1)^3}. \quad (109)$$

From normalization of the propagator we know  $\bar{\zeta}_c(0) = 1$ . Additionally, odd derivatives at the origin are 0,  $\bar{\zeta}_c'(0) = 0$ . Finally, from Eq.97 we have

$$\bar{\zeta}_c''(0) = \frac{-\langle s_c^2 \rangle}{d}. \quad (110)$$

Thus,

$$\langle r^2 C_c(r) \rangle = \frac{\langle s_c^2 \rangle}{(1 - c)^2}. \quad (111)$$

With the two moments in Eqs. (108) and (111), Eq.(106) gives the full diffusion approximation

$$C_c(r) \approx \frac{1}{1-c} m_d \left( \sqrt{\frac{\langle s_c^2 \rangle}{2d(1-c)}}, r \right). \quad (112)$$

This is then the Green's function for the diffusion equation for collision rate density under correlated emission

$$-D_{C_c} \nabla^2 C_c(\mathbf{x}) + \frac{1}{1-c} C_c(\mathbf{x}) = Q_c(\mathbf{x}) \quad (113)$$

with diffusion constant

$$D_{C_c} = \frac{v^2}{\langle r^0 C_c(r) \rangle} = \frac{\langle s_c^2 \rangle}{2d}. \quad (114)$$

It was previously conjectured [Asadzadeh and Larsen 2008] that the diffusion constant has a dimensional-dependence of  $\frac{1}{d}$ , which we previously proved for the case of exponential free paths and conjectured to hold for the case of general free-path distribution [d'Eon 2013]. We have proven this conjecture here and in the following derivations we find it also holds for uncorrelated emission and for moment-preserving diffusion approximations of the scalar flux as well.

We also generalize the approach of Grosjean [1956a] of separating the density of first collisions from the multiply-scattered portion and only using the diffusion mode for approximating the latter. The density of initial collisions has a simple analytic form and, further, it corresponds precisely to the portion of the total vector collision rate density (for particles entering collisions) that is singular in angle—in direct conflict with the angular smoothness of diffusion solutions. For these reasons, Grosjean chose to separate transport quantities into two parts, approximating one with a diffusion equation and handling the initial collision rates and uncollided flux directly, noting improved accuracy in many cases for calculations involving high absorption levels and in locations near sources and boundaries. Further details on his findings and application of the approach to convex bounded domains can be found in [Grosjean 1956a; Grosjean 1956b; Grosjean 1958a; Grosjean 1958b].

To form the diffusion approximation for the multiply-collided collision density

$$G(r) = C_c(r) - \frac{p_c(r)}{\Omega_d(r)}, \quad (115)$$

we require the expected number of multiple collisions which, given that the first collision always happens with probability 1, is

$$\langle r^0 G(r) \rangle = \frac{1}{1-c} - 1 = \frac{c}{1-c}. \quad (116)$$

The second moment is found via Eq.(52) and (97),

$$\langle r^2 G(r) \rangle = -d \frac{\partial^2}{\partial z^2} \left[ \frac{c (\bar{\xi}_c(z))^2}{1 - c \bar{\xi}_c(z)} \right]_{z=0} = \frac{(2-c)c \langle s_c^2 \rangle}{(1-c)^2}, \quad (117)$$

giving the complete approximation,

$$C_c(r) \approx \frac{p_c(r)}{\Omega_d(r)} + \frac{c}{1-c} m_d \left( \sqrt{\frac{(2-c)\langle s_c^2 \rangle}{2d(1-c)}}, r \right). \quad (118)$$

### 5.3.2 Uncorrelated emission

The case of uncorrelated emission is treated in a similar fashion. The normalization of the uncorrelated free-path distribution gives  $\bar{\zeta}_u(0) = 1$ . Combining Eqs.(90) and (97) gives

$$\bar{\zeta}_u''(0) = \frac{-\langle s_c^3 \rangle}{3\langle s_c \rangle d}. \quad (119)$$

Using Eqs.(53) we find

$$\langle r^2 C_u(r) \rangle = \frac{3c\langle s_c \rangle \langle s_c^2 \rangle + \langle s_c^3 \rangle (1-c)}{3(1-c)^2 \langle s_c \rangle}. \quad (120)$$

Thus, the classical diffusion approximation for uncorrelated emission is

$$C_u(r) \approx \frac{1}{1-c} m_d \left( \sqrt{\frac{3c\langle s_c \rangle \langle s_c^2 \rangle + \langle s_c^3 \rangle (1-c)}{6d\langle s_c \rangle (1-c)}}, r \right). \quad (121)$$

From Eq.(54) we find

$$\langle r^2 G(r) \rangle = \frac{c(3\langle s_c \rangle \langle s_c^2 \rangle + \langle s_c^3 \rangle (1-c))}{3(1-c)^2 \langle s_c \rangle} \quad (122)$$

giving the Grosjean-form approximation,

$$C_u(r) \approx \frac{p_u(r)}{\Omega_d(r)} + \frac{c}{1-c} m_d \left( \sqrt{\frac{3\langle s_c \rangle \langle s_c^2 \rangle + \langle s_c^3 \rangle (1-c)}{6d\langle s_c \rangle (1-c)}}, r \right). \quad (123)$$

## 5.4 Fluence / Scalar Flux

For the case of scalar flux we take a similar approach but preserve the first two even spatial moments of a different physical transport quantity, the scalar flux, which is not generally proportional to the collision rate density.

### 5.4.1 Correlated emission

In the case of correlated emission, the track-lengths of all segments in the random walk have the same expected value  $\langle s_c \rangle$  and are all independent random variables. The 0th moment of the scalar flux is simply the expected track-length of the entire walk over all space. With survival probability  $0 < c < 1$  at each collision, the expected number of path segments in the walk is  $1/(1-c)$ , each with a mean length of  $\langle s_c \rangle$ , thus the 0th moment of the scalar flux is simply

$$\langle r^0 \phi_c(r) \rangle = \frac{\langle s_c \rangle}{1-c}. \quad (124)$$

While the scalar flux and collision rate density do not generally exhibit the classical proportionality, we see that in the case of correlated emission in infinite media the 0th moment of the two quantities does show a familiar form,

$$\frac{\langle r^0 C_c(r) \rangle}{\langle r^0 \phi_c(r) \rangle} = \frac{1}{\langle s_c \rangle}. \quad (125)$$

The complete approximations for correlated flux are found most readily from Eq. 61, with the same diffusion lengths as the case of uncorrelated collision density, and a scale factor of  $\langle s_c \rangle$ , producing the classical-form diffusion approximation

$$\phi_c(r) \approx \frac{\langle s_c \rangle}{1-c} m_d \left( \sqrt{\frac{3c\langle s_c \rangle \langle s_c^2 \rangle + \langle s_c^3 \rangle (1-c)}{6d\langle s_c \rangle (1-c)}}, r \right). \quad (126)$$

and the Grosjean-form approximation

$$\phi_c(r) \approx \frac{X_c(r)}{\Omega_d(r)} + \frac{c\langle s_c \rangle}{1-c} m_d \left( \sqrt{\frac{3\langle s_c \rangle \langle s_c^2 \rangle + \langle s_c^3 \rangle (1-c)}{6d\langle s_c \rangle (1-c)}}, r \right). \quad (127)$$

#### 5.4.2 Uncorrelated emission

In the case of uncorrelated emission, the expected track-length of the entire path is

$$\langle r^0 \phi_u(r) \rangle = \langle r^0 \phi_c(r) \rangle - \langle s_c \rangle + \langle s_u \rangle = \frac{c\langle s_c \rangle}{1-c} + \frac{\langle s_c^2 \rangle}{2\langle s_c \rangle}, \quad (128)$$

which is the mean total track-length for correlated emission with the correlated free-path mean for the initial step removed and replaced with the uncorrelated mean for that emission step. The second moment can be determined from Eqs.(62) and (97)

$$\begin{aligned} \langle r^2 \phi_u(r) \rangle &= -d \frac{\partial^2}{\partial z^2} \left[ \bar{\chi}_u(z) + \bar{\chi}_c(z) c \frac{\bar{\xi}_u(z)}{1-c\bar{\xi}_c(z)} \right]_{z=0} = \\ &= -d \left( \frac{c^2 \bar{\chi}_c(0) \bar{\xi}_c''(0)}{(1-c)^2} + \frac{c (\bar{\chi}_c(0) \bar{\xi}_u''(0) + \bar{\chi}_c''(0))}{1-c} + \bar{\chi}_u''(0) \right) \end{aligned} \quad (129)$$

where here we have used  $\bar{\xi}_c'(0) = \bar{\chi}_c'(0) = 0$  and  $\bar{\xi}_c(0) = \bar{\xi}_u(0) = 1$  to simplify. From Eqs.(91) we also have

$$\bar{\chi}_c''(0) = \frac{-\langle s_c^3 \rangle}{3d} \quad (130)$$

$$\bar{\chi}_u''(0) = \frac{-\langle s_c^4 \rangle}{12\langle s_c \rangle d} \quad (131)$$

From Eq.(87) we have  $\bar{\chi}_c(0) = \langle s_c \rangle$  and we can reduce Eq.(129) to

$$\langle r^2 \phi_u(r) \rangle = \frac{1}{12} \left( \frac{4c(3c\langle s_c \rangle \langle s_c^2 \rangle - 2c\langle s_c^3 \rangle + 2\langle s_c^3 \rangle)}{(1-c)^2} + \frac{\langle s_c^4 \rangle}{\langle s_c \rangle} \right) \quad (132)$$

giving the full diffusion approximation

$$\phi_u(r) \approx \left( \frac{c\langle s_c \rangle}{1-c} + \frac{\langle s_c^2 \rangle}{2\langle s_c \rangle} \right) m_d \left( \sqrt{\frac{4c(3c\langle s_c \rangle \langle s_c^2 \rangle - 2c\langle s_c^3 \rangle + 2\langle s_c^3 \rangle) + \frac{\langle s_c^4 \rangle}{\langle s_c \rangle}}{(1-c)^2} + \frac{\langle s_c^2 \rangle}{2\langle s_c \rangle}}, r \right). \quad (133)$$

Finally, a straightforward calculation similar to the previous gives the Grosjean-form approximation,

$$\phi_u(r) \approx \frac{X_u(r)}{\Omega_d(r)} + \frac{c\langle s_c \rangle}{1-c} m_d \left( \sqrt{\frac{3c\langle s_c \rangle \langle s_c^2 \rangle + 2\langle s_c^3 \rangle (1-c)}{6d\langle s_c \rangle (1-c)}}, r \right). \quad (134)$$

## 5.5 Anisotropic Scattering

For simplicity, we have so far considered only isotropic scattering. The Fourier-transform approach used in this section can be extended for the case of anisotropic scattering (persistent random walks) using the methods outlined by Grosjean [1951; 1953], but is considerably more involved. For the case of collision rate about a correlated source, however, the required moments are known and we briefly review them here for completeness and to relate to previous work.

### 5.5.1 Classical Diffusion Approximation for Anisotropic Scattering

As noted previously, the 0th moment of the collision rate is invariant to phase function,

$$\langle r^0 C_c(r) \rangle = \frac{1}{1-c}. \quad (135)$$

For random flights in Flatland with a general, symmetric phase function having mean cosine  $-1 \leq g \leq 1$  the second moment of the  $n$ th collision is [Hall 1977; Kareiva and Shigesada 1983]

$$\langle r^2 C_c(r|n) \rangle = n\langle s_c^2 \rangle + \frac{g}{1-g} 2\langle s_c \rangle^2 \left( n - \frac{1-g^n}{1-g} \right), \quad (136)$$

from which we can sum over all orders and introduce absorption to find

$$\langle r^2 C_c(r) \rangle = \sum_{n=1}^{\infty} c^{n-1} \langle r^2 C_c(r|n) \rangle = \frac{\langle s_c^2 \rangle}{(1-c)^2} \left( 1 + cg \frac{2\langle s_c \rangle^2}{\langle s_c^2 \rangle (1-cg)} \right). \quad (137)$$

Equation 137 agrees with a previous derivation for the case of exponential random flights in 3D [Grosjean 1963a]<sup>8</sup> and is consistent with 2D and 3D results in plane geometry [Gandjbakhche et al. 1992]. We suspect that Equation 137 holds generally in  $dD$ .

<sup>8</sup> Grosjean [1963a] (p.26) derives moment expressions for exponential free flights in 3D with general phase function including  $\langle r^6 C_c(r) \rangle$  and  $\langle r^8 C_c(r) \rangle$ , but we find the latter expression to not match MC.

Combining the two moments with Equation 106, we find the diffusion coefficient for correlated-emission collision rate generalizing Equation 114 to anisotropic scattering,

$$D_{C_c} = \frac{v^2}{\langle r^0 C_c(r) \rangle} = \frac{\langle s_c^2 \rangle}{2d} \left( 1 + cg \frac{2\langle s_c \rangle^2}{\langle s_c^2 \rangle (1 - cg)} \right). \quad (138)$$

The scaling of a classical anisotropically-scattering media to an isotropically-scattering one based on the reduced scattering coefficient  $\Sigma'_s = \Sigma_s(1 - g)$ , preserves the diffusion coefficient  $D_{C_c}$ . This is known not to hold generally with nonexponential free paths [Gandjbakhche et al. 1992], but GRT offers a much richer set of potential similarity relations by varying the free-path distribution as a whole, and not just its mean, and is an interesting area for future work.

### 5.5.2 Grosjean Diffusion Approximation for Anisotropic Scattering

For completeness, we include the Grosjean-form approximation for anisotropic scattering. The 0th moment of the multiply-collided collision density remains

$$\langle r^0 G(r) \rangle = \frac{1}{1 - c} - 1 = \frac{c}{1 - c}. \quad (139)$$

The second moment is found from the Neumann series of the classical derivation above, removing the 1st term,

$$\langle r^2 G(r) \rangle = \sum_{n=2}^{\infty} c^{n-1} \langle r^2 C_c(r|n) \rangle = \frac{\langle s_c^2 \rangle}{(1 - c)^2} \left( 1 + cg \frac{2\langle s_c \rangle^2}{\langle s_c^2 \rangle (1 - cg)} \right) - \langle s_c^2 \rangle \quad (140)$$

giving the complete approximation,

$$C_c(r) \approx \frac{p_c(r)}{\Omega_d(r)} + \frac{c}{1 - c} m_d \left( \sqrt{\frac{(2 - c)\langle s_c^2 \rangle (1 - cg) + 2g\langle s_c \rangle^2}{2(1 - c)d(1 - cg)}}, r \right). \quad (141)$$

### 5.5.3 Related Parameter-Of-Smallness Diffusion Derivations

Using a parameter-of-smallness asymptotic analysis, Larsen and Vasques [2011] derived a diffusion coefficient in 3D for the scalar flux for correlated emission that is related to Equation 138 by classical proportionality,  $D_{\phi_c} = D_{C_c}/\langle s_c \rangle$ , and so is not a moment-preserving approximation for the flux in general. Frank and Goudon [2010] derived a similar diffusion coefficient for general dimension  $d$  that is the same as Larsen's when  $c = 1$ . Exactly why these derivations preserve collision rate moments and not flux moments is not clear to us, but we suspect it relates to the transformed quantity in (6.4) of Larsen [2007] that scales flux by the equilibrium distribution of free paths. This scaling includes the inverse mean free path  $1/\langle s_c \rangle$  which, in the classical case, converts the flux to a collision rate and also has a  $O(\varepsilon^{-1})$  scaling. Frank and Goudon's result was also found by Rukolaine [2016]. From a moment-preserving perspective (but for collision-rate, not flux), the absorption-dependent diffusion coefficient would seem to be preferred.

To illustrate the potential severity of the mismatch between collision rate and flux asymptotics, consider correlated emission with the free-path distribution,

$$p_c(s) = \frac{12s}{(1+s)^5}. \quad (142)$$

With a finite mean square free path,

$$\langle s_c^2 \rangle = \int_0^\infty p_c(r)r^2 dr = 3, \quad (143)$$

the moment-preserving diffusion approximations follow and are well behaved. For the scalar flux, however, given

$$X_c(s) = 1 - \int_0^s p_c(s')ds' = \frac{4s+1}{(s+1)^4}, \quad (144)$$

we find, even for the uncollided flux alone, assuming no scattering,

$$\langle r^2 \phi(r) \rangle_{c=0} = \int_0^\infty X_c(r)r^2 dr = \infty \quad (145)$$

and so a diffusion mode cannot preserve the 2nd moment of the scalar flux. Given this difference, the flux diffusion asymptotics just mentioned [Larsen and Vasques 2011; Frank et al. 2010] are surprising.

## 5.6 Discussion and Validation

### 5.6.1 Reduction to the Classical Case

Compared to the simplicity of the classical  $P_1$  diffusion approximation, the isotropic point source diffusion Green's function for the infinite medium has a much more complicated form in the generalized case, requiring moments up to  $\langle s_c^4 \rangle$ . In the case of uncorrelated emission, the scalar flux diffusion coefficient is

$$D_{\phi_u} = \frac{v^2}{\langle r^0 \phi_u(r) \rangle} = \frac{\langle s_c \rangle (4c \langle s_c \rangle (3c \langle s_c \rangle \langle s_c^2 \rangle - 2c \langle s_c^3 \rangle + 2 \langle s_c^3 \rangle) + (1-c)^2 \langle s_c^4 \rangle)}{6d (2c \langle s_c \rangle^2 - c \langle s_c^2 \rangle + \langle s_c^2 \rangle)^2}. \quad (146)$$

This result is, however, consistent with the classical diffusion ( $P_1$ ) approximation. In the case of classical scattering with correlated free-path distribution  $p_c(s) = \Sigma_t e^{-\Sigma_t s}$ , the correlated moments are

$$\langle s_c^m \rangle = \frac{m!}{(\Sigma_t)^m} \quad (147)$$

and the diffusion coefficient (146) reduces to the well-known

$$D_{\phi_c} = D_{\phi_u} = \frac{(1-c)^2}{\Sigma_t d} + \frac{(2-c)c}{\Sigma_t d} = \frac{1}{\Sigma_t d} \quad (148)$$

with the portion  $(1-c)^2/(\Sigma_t d)$  arising from the uncollided flux and  $(2-c)c/(\Sigma_t d)$  from the collided portion.

While there are effectively four forms of moment-preserving diffusion asymptotics in GRT, with two having identical decay rates, there is at most one asymptotic decay rate

of the “rigorous diffusion” nature, corresponding to the largest real eigenvalue (if one exists) of the collision kernel, a zero of the dispersion function [d’Eon 2013]

$$\Lambda(z) = 1 - c\bar{\zeta}_c(i/z), \quad (149)$$

which is a common denominator in all four frequency-space Green’s function representations.

### 5.6.2 Power-Law Attenuation

We now consider the case of transport with a power-law attenuation law as defined earlier in Section 3.4.2. The full set of moments required for the diffusion approximations are

$$\langle s_c \rangle = \ell, \quad (150)$$

$$\langle s_c^2 \rangle = \ell^2 \frac{2a}{a-1}, \quad (151)$$

$$\langle s_c^3 \rangle = \ell^3 \frac{6a^2}{a^2 - 3a + 2}, \quad (152)$$

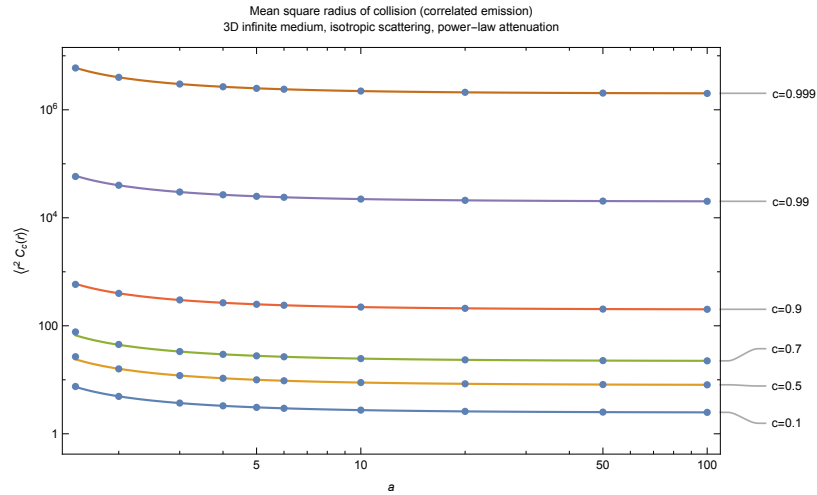
$$\langle s_c^4 \rangle = \ell^4 \frac{24a^4(a+1)\Gamma(a-3)}{\Gamma(a+2)} \quad (153)$$

with the restrictions  $a > m - 1$  for moment  $\langle s_c^m \rangle$ .

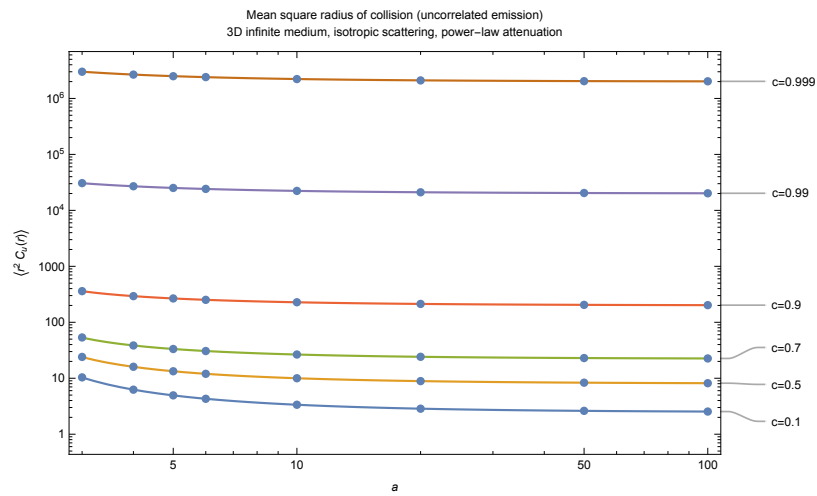
We performed a suite of Monte Carlo simulations for power-law transport with unit mean correlated free path ( $\langle s_c \rangle = \ell = 1$ ) about an isotropic point source in infinite 3D medium configurations. For both the collision rate density and scalar flux we estimated tallies of both the radial quantities as well as their 2nd radial moments, all using an analog collision estimator. For the moments, we compared Monte Carlo and deterministic predictions and found agreement in all cases. For the collision density case, the Monte Carlo validation of Eqs.(111) and (120) is summarized in Figure 9. Likewise, Figure 10 summarizes the validation of Eqs.(120) and (132) for the scalar flux moments.

A comprehensive evaluation of the accuracy of the generalized diffusion approximations over a wide variety of free-path distributions is beyond the scope of the current work. We briefly highlight some of our findings for the case of power-law transport and note several trends. In a future part of this work we hope to expand upon this accuracy evaluation in the context of method-of-images application of these approximations to solve the searchlight problem in the style of [d’Eon and Irving 2011].

Figures 11 and 12 show the performance of the diffusion and Grosjean-form diffusion approximations for collision rate density ( $C_c(r)$  and  $C_u(r)$ ), and scalar flux  $\phi_u(r)$ . By Eq.(61) the evaluation of  $\phi_c(r)$  is equivalent to that of  $C_u(r)$ . Some general trends from the case of classical exponential scattering survived the generalization to power-law transport; in the short range regime  $r < 10\langle s_c \rangle$ , we noted lower overall relative error for the Grosjean-form approximation vs. the classical diffusion form in all cases. By including the first term in the Neumann series solution exactly, the Grosjean-form approaches zero error everywhere as  $c \rightarrow 0$ , whereas the classical diffusion form remains consistently poor for very low radius ( $r < \langle s_c \rangle$ ) regardless of absorption level.

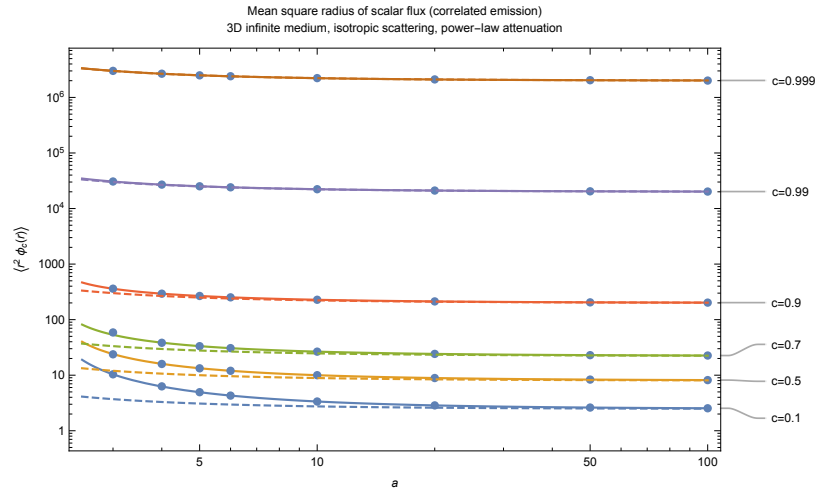


(a) Correlated emission -  $\langle r^2 C_c(r) \rangle$

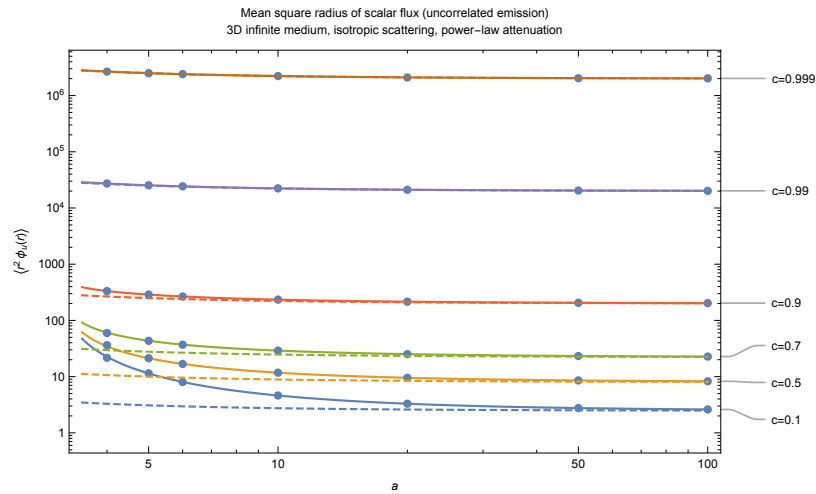


(b) Uncorrelated emission -  $\langle r^2 C_u(r) \rangle$

**Figure 9:** Mean square distance of collision in 3D for power-law transport: Monte Carlo (dots) vs. deterministic (continuous).



(a) Correlated emission -  $\langle r^2 \phi_c(r) \rangle$



(b) Uncorrelated emission -  $\langle r^2 \phi_u(r) \rangle$

**Figure 10:** Mean square scalar flux in 3D for power-law transport: Monte Carlo (dots) vs. deterministic (continuous). The moments for collision rate density are shown (dashed) for comparison.

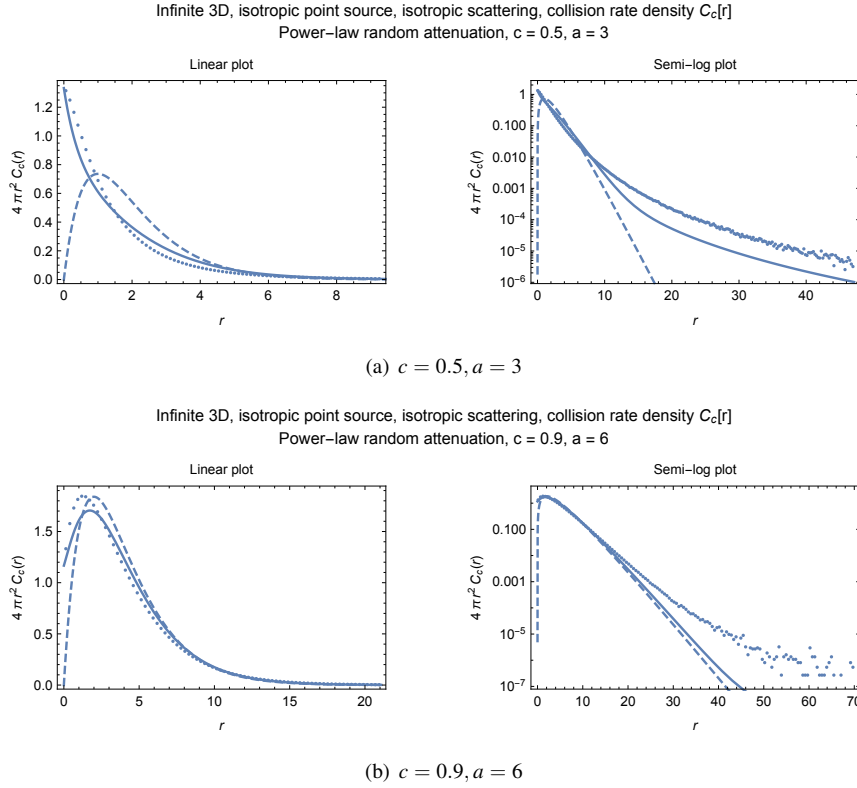


**Figure 11:** Collision-rate density  $C_c(r)$  about an correlated-emission isotropic point as predicted by Monte Carlo (dots), diffusion approximation (dashed) and Grosjean-form diffusion approximation (continuous).

For absorption levels in the range  $0.5 < c < 0.9$  we saw five times less relative error for  $r < 10\langle s_c \rangle$  in the Grosjean case vs the classical case for near-classical transport ( $a > 50$ ), with the Grosjean advantage shrinking to only a 20% reduction in relative error when  $a = 4$ .

For absorption levels  $c \leq 0.99$  we also noted a raised tail that is missing from the classical diffusion approximation and not a property of classical transport. We attribute this to the free path distribution approaching a heavy-tailed distribution as  $a \rightarrow 0$ , with fewer bounded moments as  $a$  decreases, thereby presenting an increasing challenge to the diffusion approximation as  $a$  decreases. This raised tail occurs at all absorption levels  $c < 1$ . The uncollided term alone, having a power-law falloff, will eventually dominate any exponential, but it was not observable in an analog simulation at  $c = 0.999$  with only  $10^6$  histories. The Grosjean-form approximation includes this bent tail, by including the power-law uncollided term exactly, but the relative error at these distances is seen to be as much as an order of magnitude.

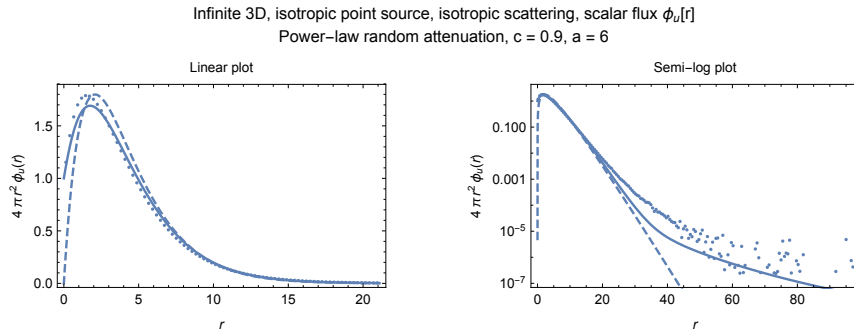
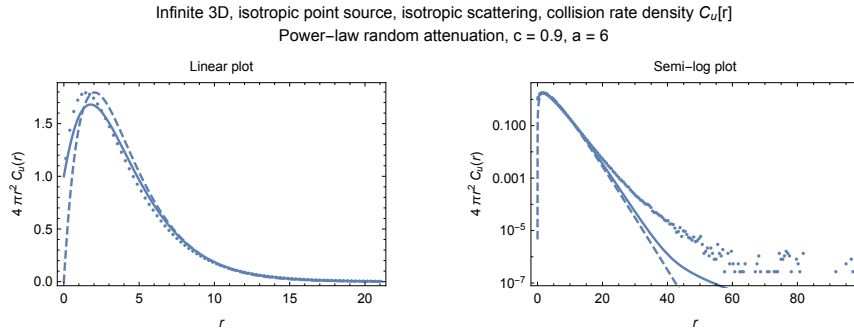


**Figure 12:** (a) Collision-rate density  $C_u(r)$  and (b) scalar flux  $\phi_u(r)$  for the case of uncorrelated emission from an isotropic point source in an infinite 3D medium with power-law attenuation with unit correlated mean free path  $\langle s_c \rangle = \ell = 1$ . Predictions by Monte Carlo (dots), diffusion approximation (dashed) and Grosjean-form diffusion approximation (continuous).

## 6 Discussion and Outlook

Under a theme of exploring the non-local proportionality between the density of particles in flight to the rate at which that flight leads to collisions, we have proposed new generalized Monte Carlo estimators, Green’s functions and diffusion approximations for generalized linear Boltzmann transport. An equilibrium imbedding of Larsen and Vasques’s [2011] framework into bounded domains has required pairs of solutions in most cases, which were previously equivalent in the classical theory, and special handling of the two classes of free-paths throughout. We distinguished between flux-proportional and collision-rate-proportional estimations and defined the analog walk for GRT.

We found Larsen’s formulation of GRT via  $\Sigma_t(s)$  very powerful, making it straightforward to bring much of the machinery of classical Monte Carlo methods to bear. Adjoint estimation, importance, and the complexity of bidirectional estimators [Veach 1997; Krycki 2015; Vitali et al. 2018] and linear combinations of many forms of different estimators [Křivánek et al. 2014] has been left for future work.

We have preferred the integral form of the transport equation in GRT, wherever possible, to avoid handling  $\psi(\mathbf{x}, \vec{\omega}, s)$  directly. There are, however, some important cases we have not discussed where it would seem  $\psi(\mathbf{x}, \vec{\omega}, s)$  is unavoidable. To extend the condensed-history acceleration scheme of Fleck and Canfield [1984], which uses pre-computed or analytic scattering solutions in finite spherical domains, requires a notion of a virtual boundary in GRT—a boundary across which correlation is maintained. In jumping to the surface of the virtual sphere boundary and carrying on the transport from there, knowledge of  $\psi(\mathbf{x}, \vec{\omega}, s)$  at the boundary is required to ensure that the balance of collisions outside of the sphere is not changed by the acceleration. This notion has been lacking from previous applications of the method to GRT [Moon et al. 2007; Meng et al. 2015; Müller et al. 2016], where  $s$  has been reset to 0 and correlated-origin free-path statistics follow each application of the accelerators. Generalizing Placzek’s Lemma [Case et al. 1953] and adding/doubling [van de Hulst 1980; Peltoniemi 1993] will also require the notion of virtual boundaries and  $\psi(\mathbf{x}, \vec{\omega}, s)$ .

Close inspection of the relationship between flux and collision rate has highlighted some subtle relationships that are often taken for granted or, occasionally, misunderstood. In light of that, there may be benefit in revisiting some classical settings with a new lens. For example, the lengthy treatment of transmittance estimation in the short form of photon beams [Jarosz et al. 2011] can be collapsed to noting simply that the track-length estimator is an unbiased estimator for the *flux* in heterogeneous classical media under delta tracking and that, needing the *collision-rate*, not flux, to send photons towards the camera, requires the track-length-collision-rate estimator. Provided that the density estimation kernel is small and the cross section is approximately constant across it, the cross-section integral can be approximated. More generally, the role of Monte Carlo methods in computer graphics might benefit from being recast as fundamentally placing less importance on flux in scattering volumes and more importance on collision rate, moving away from a notion of transmittance estimation to one of collision-rate estimation. Transmittance estimation seems only relevant in graphics

at a camera sensor or on the surface of a light during next-event estimation, neither of which involve scoring along a track-length.

There would appear to be great promise for solving plane-parallel problems with isotropic scattering in GRT by generalizing the Schwarzschild-Milne kernel for the scalar collision density to

$$K_C(x) = \frac{c}{2} \int_0^1 p_c(|x|/\mu) \frac{1}{\mu} d\mu, \quad (154)$$

and solving a Fredholm integral equation of the second kind with a kernel that is no longer  $E_1(|x|)$ . The approach is then nearly identical to that of problems with complete frequency redistribution, and the Wiener-Hopf equations have been solved in the general case [Mullikin 1968; Ivanov 1994]. In part 4 of this work we treat bounded plane-parallel problems in detail with a particular focus on the Gamma-2 free-path distribution. Part 5 will explore approximate deterministic solutions of searchlight problems utilizing the method of images.

## 6.1 Limitations

The present assumption of path-length independence on single-scattering albedo limits the scope of application to random media where absorption and scattering occur from the same correlated structure. This would not be an appropriate assumption of, say, metallic sphere packings in a paint layer, where absorption occurs in the substrate that holds the spheres, because the single-scattering albedo in this scenario would depend on  $s$  (the equivalence theorem [van de Hulst 1980] does not hold in GRT). This calls into question the application of this form of GRT to tissue optics [Wrenninge et al. 2017] where scattering is primarily caused by random changes of index of refraction in the cellular tissue structures, while absorption is primarily caused by independent distributions of melanin and hemoglobin chromophores [Wang 2000; Tuchin 2007]. We remark that it is straightforward to extend much of the current presentation to include correlated scattering that is imbedded in a classical, purely-absorbing substrate with absorption coefficient  $\Sigma_a$ . An additional, reciprocal attenuation  $e^{-\Sigma_a s}$  is added to the Monte Carlo estimators to treat the substrate absorption in the expected-value manner. Extension of the Fourier derivation of Green's function is less straightforward, however, and we leave this for future work. Extending the methods of the present paper to a fully general GRT framework of path-length dependent absorption [Rukolaine 2016] phase function [Jarabo et al. 2018] and support for anomalous diffusion [Liemert and Kienle 2017] would be a much larger task and the conditions for Helmholtz reciprocity in such settings are not immediately obvious.

There is also important open work to relate a given model in GRT to a scale at which it can be safely assumed that no explicit structure would be resolved in imaging that media at that distance, making the bulk statistical model an appropriate choice.

A comprehensive notion of heterogeneity in GRT (non-uniform mean density) is also an interesting open question, given that optical path-length stretching [Bitterli et al. 2018] would not be able to avoid also stretching density-invariant aspects of correla-

tion. Consider, for example, monodisperse hard sphere packings in a medium where the average number density of spheres changes continuously with position. The restriction of non-intersection is not a function of the local number density and does not scale in the sense of the traditional optical depth.

Invariant properties of general random walks [Frisch and Frisch 1995; Mazzolo et al. 2014] provide additional benchmarking tools for both Monte Carlo and deterministic methods. Under the mental model for GRT described in Section 3.3.2 it seems intuitive that the beginning of an uncorrelated free path involves all random realizations in equilibrium and that, therefore, the macroscopic cross-section beginning that walk should be related to the number densities  $\rho_i$  and constituent cross-sections  $\sigma_i$  in the classical atomic-mix sense, independent of correlation,

$$\Sigma_{tu}(0) = \sum_i \rho_i(\mathbf{x}) \sigma_i. \quad (155)$$

We have observed that this property holds in the blue noise GRT model previously proposed [d’Eon 2018], in Davis’s power-law model [Davis and Mineev-Weinstein 2011], and for Markovian binary mixtures (presented in the next paper), but, without further evidence, we leave this as a conjecture for now.

## 7 Conclusion

We have presented new Monte Carlo and deterministic methods for nonclassical linear transport and related stochastic processes. The collision estimator for collision rate and the track-length estimator for flux both have been shown to remain equivalent to the classical case, with each estimator requiring path-length-dependent scores when estimating the opposite quantity (summarized in Figure 2). Limitations of the collision estimator for flux estimation in negatively-correlated media have been identified and a new family of estimators based on fictitious scattering has been introduced to mitigate these limitations.

The Monte Carlo estimators have been verified using new Green’s function derivations for point and plane sources in infinite media, extending Grosjean’s random flight solutions to include the transmittance kernel for flux and a unique PDF for uncorrelated-origin free paths in a unified manner. Algebraic equations for the related moment-preserving diffusion approximations have also been derived, requiring moments up to order 4 in some cases. We have presented the first generalized moment-preserving diffusion asymptotics for scalar flux and have shown that previous asymptotics correspond to classically-scaled asymptotics for the collision rate.

## 8 Acknowledgements

I am indebted to M.M.R. Williams for introducing me to the work of Larsen and Vasques and for his encouragement of the present work. Discussions of transport and memory with Barry Ganapol, Wenzel Jakob, Steve Marschner and Anthony Davis were also very helpful. I also need to thank Todd Urbatsch for pointing me to the work of

Fleck and Canfield [1984], Eric Heitz for mentioning the work of Savo et al. [2017], Andrea Zoia for his thorough review of an early revision and the anonymous referees for their help improving the presentation.

## References

- ALT, W. 1980. Biased random walk models for chemotaxis and related diffusion approximations. *Journal of mathematical biology* 9, 2, 147–177. <https://doi.org/10.1007/BF00275919>.
- AMBOS, A. Y., AND MIKHAILOV, G. 2011. Statistical simulation of an exponentially correlated many-dimensional random field. *Russian Journal of Numerical Analysis and Mathematical Modelling* 26, 3, 263–273. <https://doi.org/10.1515/rjnamm.2011.014>.
- APRESYAN, L., AND KRAVTSOV, Y. 1996. *Radiation Transfer - Statistical and Wave Aspects*. Gordon and Breach.
- ARRIDGE, S. 1999. Optical tomography in medical imaging. *Inverse problems* 15, 2, R41. <https://doi.org/10.1088/0266-5611/15/2/022>.
- ASADZADEH, M., AND LARSEN, E. 2008. Linear transport equations in Flatland with small angular diffusion and their finite element approximations. *Mathematical and Computer Modelling* 47, 3-4, 495–514. <https://doi.org/10.1016/j.mcm.2007.05.004>.
- AUDIC, S., AND FRISCH, H. 1993. Monte-Carlo simulation of a radiative transfer problem in a random medium: Application to a binary mixture. *Journal of Quantitative Spectroscopy and Radiative Transfer* 50, 2, 127–147. [https://doi.org/10.1016/0022-4073\(93\)90113-V](https://doi.org/10.1016/0022-4073(93)90113-V).
- BANKO, A. J., VILLAFANE, L., KIM, J. H., ESMAILY, M., AND EATON, J. K. 2019. Stochastic modeling of direct radiation transmission in particle-laden turbulent flow. *Journal of Quantitative Spectroscopy and Radiative Transfer*. <https://doi.org/10.1016/j.jqsrt.2019.01.005>.
- BARABANENKOV, Y. N., AND FINKEL'BERG, V. M. 1968. Radiation transport equation for correlated scatterers. *Sov. Phys. JETP* 26, 3, 587–591. [http://www.jetp.ac.ru/cgi-bin/dn/e\\_026\\_03\\_0587.pdf](http://www.jetp.ac.ru/cgi-bin/dn/e_026_03_0587.pdf).
- BARDSLEY, J., AND DUBI, A. 1981. The average transport path length in scattering media. *SIAM Journal on Applied Mathematics* 40, 1, 71–77. <https://doi.org/10.1137/0140005>.
- BARTHELEMY, P., BERTOLOTTI, J., AND WIERSMA, D. S. 2008. A Lévy flight for light. *Nature* 453, 7194, 495–498. <https://doi.org/10.1038/nature06948>.
- BECKER, B., KOPECKY, S., HARADA, H., AND SCHILLEBEECKX, P. 2014. Measurement of the direct particle transport through stochastic media using neutron

- resonance transmission analysis. *The European Physical Journal Plus* 129, 4, 58. <https://doi.org/10.1140/epjp/i2014-14058-6>.
- BINZONI, T., MARTELLI, F., AND KOZUBOWSKI, T. J. 2018. Generalized time-independent correlation transport equation with static background: influence of anomalous transport on the field autocorrelation function. *JOSA A* 35, 6, 895–902. <https://doi.org/10.1364/JOSAA.35.000895>.
- BITTERLI, B., RAVICHANDRAN, S., MÜLLER, T., WRENNINGE, M., NOVÁK, J., MARSCHNER, S., AND JAROSZ, W. 2018. A radiative transfer framework for non-exponential media. *ACM Transactions on Graphics* 37, 6. <https://doi.org/10.1145/3272127.3275103>.
- BLANCO, S., AND FOURNIER, R. 2003. An invariance property of diffusive random walks. *EPL (Europhysics Letters)* 61, 2, 168. <https://doi.org/10.1209/epl/i2003-00208-x>.
- BOISSÉ, P. 1990. Radiative transfer inside clumpy media-The penetration of UV photons inside molecular clouds. *Astronomy and Astrophysics* 228, 483–502. <http://adsabs.harvard.edu/abs/1990A%26A...228..483B>.
- BOROVOI, A. G. 2006. Multiple scattering of short waves by uncorrelated and correlated scatterers. In *Light scattering reviews*. Springer, 181–252.
- CASE, K. M., AND ZWEIFEL, P. F. 1967. *Linear Transport Theory*. Addison-Wesley.
- CASE, K. M., DE HOFFMAN, F., AND PLACZEK, G. 1953. *Introduction to the Theory of Neutron Diffusion*, vol. 1. US Government Printing Office.
- CHANDRASEKHAR, S. 1960. *Radiative Transfer*. Dover.
- DAVIS, A. B., AND MINEEV-WEINSTEIN, M. B. 2011. Radiation propagation in random media: From positive to negative correlations in high-frequency fluctuations. *Journal of Quantitative Spectroscopy and Radiative Transfer* 112, 4, 632–645. <https://doi.org/10.1016/j.jqsrt.2010.10.001>.
- DAVIS, A. B., AND XU, F. 2014. A generalized linear transport model for spatially correlated stochastic media. *Journal of Computational and Theoretical Transport* 43, 1-7, 474–514. <https://doi.org/10.1080/23324309.2014.978083>.
- DAVIS, A., MARSHAK, A., WISCOMBE, W., AND CAHALAN, R. 1996. Scale invariance of liquid water distributions in marine stratocumulus. Part I: Spectral properties and stationarity issues. *Journal of the atmospheric sciences* 53, 11, 1538–1558. [https://doi.org/10.1175/1520-0469\(1996\)053<1538:SIOLWD>2.0.CO;2](https://doi.org/10.1175/1520-0469(1996)053<1538:SIOLWD>2.0.CO;2).
- DAVIS, A. B. 2006. Effective propagation kernels in structured media with broad spatial correlations, illustration with large-scale transport of solar photons through cloudy atmospheres. In *Computational Methods in Transport*. Springer, 85–140. [https://doi.org/10.1007/3-540-28125-8\\_5](https://doi.org/10.1007/3-540-28125-8_5).

- DAVISON, B. 1957. *Neutron Transport Theory*. Oxford University Press.
- DE GREGORIO, A., AND ORSINGHER, E. 2012. Flying randomly in rd with dirichlet displacements. *Stochastic processes and their applications* 122, 2, 676–713. <https://doi.org/10.1016/j.spa.2011.10.009>.
- DE GREGORIO, A. 2012. On random flights with non-uniformly distributed directions. *Journal of Statistical Physics* 147, 2, 382–411. [https://doi.org/10.1016/0306-4549\(92\)90013-2](https://doi.org/10.1016/0306-4549(92)90013-2).
- DE GREGORIO, A. 2017. A note on isotropic random flights moving in mixed poisson environments. *Statistics & Probability Letters* 129, 311–317. <https://doi.org/10.1016/j.spl.2017.06.021>.
- DE MULATIER, C., MAZZOLO, A., AND ZOIA, A. 2014. Universal properties of branching random walks in confined geometries. *EPL (Europhysics Letters)* 107, 3, 30001. <https://doi.org/10.1209/0295-5075/107/30001>.
- D'EON, E., AND IRVING, G. 2011. A quantized-diffusion model for rendering translucent materials. In *ACM Transactions on Graphics (TOG)*, vol. 30, ACM, 56. <https://doi.org/10.1145/1964921.1964951>.
- D'EON, E. 2013. Rigorous Asymptotic and Moment-Preserving Diffusion Approximations for Generalized Linear Boltzmann Transport in Arbitrary Dimension. *Transport Theory and Statistical Physics* 42, 6-7, 237–297. <https://doi.org/10.1080/00411450.2014.910231>.
- D'EON, E. 2014. A dual-beam 3d searchlight bssrdf. *ACM SIGGRAPH 2014 Talks* 65, 1, 1. <http://doi.acm.org/10.1145/2614106.2614140>.
- D'EON, E. 2018. A reciprocal formulation of nonexponential radiative transfer. 1: Sketch and motivation. *Journal of Computational and Theoretical Transport*. <https://doi.org/10.1080/23324309.2018.1481433>.
- DONNER, C., AND JENSEN, H. W. 2005. Light diffusion in multi-layered translucent materials. *ACM Trans. Graphic.* 24, 3, 1032–1039. <https://doi.org/10.1145/1186822.1073308>.
- DUDERSTADT, J., AND MARTIN, W. 1979. *Transport theory*. Wiley-Interscience.
- DUNN, W. L. 1985. The back-projection angular flux estimator. *Journal of Computational Physics* 61, 3, 391–402. [https://doi.org/10.1016/0021-9991\(85\)90071-3](https://doi.org/10.1016/0021-9991(85)90071-3).
- DUTKA, J. 1985. On the problem of random flights. *Archive for history of exact sciences* 32, 3, 351–375. <https://doi.org/10.1007/BF00348451>.
- DWIVEDI, S. 1982. A new importance biasing scheme for deep-penetration Monte Carlo. *Annals of Nuclear Energy* 9, 7, 359–368. [https://doi.org/10.1016/0306-4549\(82\)90038-X](https://doi.org/10.1016/0306-4549(82)90038-X).

- FARRELL, T. J., PATTERSON, M. S., AND WILSON, B. 1992. A diffusion theory model of spatially resolved, steady-state diffuse reflections for the noninvasive determination of tissue optical properties *in vivo*. *Med. Phys.* 19, 4, 879–888. <https://doi.org/10.1118/1.596777>.
- FLECK, J., AND CANFIELD, E. 1984. A random walk procedure for improving the computational efficiency of the implicit Monte Carlo method for nonlinear radiation transport. *Journal of Computational Physics* 54, 3, 508–523. [https://doi.org/10.1016/0021-9991\(84\)90130-X](https://doi.org/10.1016/0021-9991(84)90130-X).
- FRANK, M., GOUDON, T., ET AL. 2010. On a generalized Boltzmann equation for non-classical particle transport. *Kinetic and Related Models* 3, 395–407. <https://doi.org/10.3934/krm.2010.3.395>.
- FRANK, M., KRYCKI, K., LARSEN, E. W., AND VASQUES, R. 2015. The nonclassical Boltzmann equation and diffusion-based approximations to the Boltzmann equation. *SIAM Journal on Applied Mathematics* 75, 3, 1329–1345. <https://doi.org/10.1137/140999451>.
- FRANKEL, A., IACCARINO, G., AND MANI, A. 2017. Optical depth in particle-laden turbulent flows. *Journal of Quantitative Spectroscopy and Radiative Transfer* 201, 10–16. <https://doi.org/10.1016/j.jqsrt.2017.06.029>.
- FRISCH, U., AND FRISCH, H. 1995. Universality of escape from a half-space for symmetrical random walks. In *Lévy Flights and Related Topics in Physics*. Springer, 262–268. [https://doi.org/10.1007/3-540-59222-9\\_39](https://doi.org/10.1007/3-540-59222-9_39).
- FRISCH, U. 1968. Wave propagation in random media. In *Probabilistic methods in applied mathematics*, A. Bharucha-Reid, Ed. Academic Press, 75–198.
- FULGER, D., SCALAS, E., AND GERMANO, G. 2008. Monte Carlo simulation of uncoupled continuous-time random walks yielding a stochastic solution of the space-time fractional diffusion equation. *Physical Review E* 77, 2, 021122. <https://doi.org/10.1103/PhysRevE.77.021122>.
- GANAPOL, B. 2008. Analytical Benchmarks for Nuclear Engineering Applications. Tech. Rep. 6292, OECD/NEA.
- GANDJBAKHCHE, A., BONNER, R., AND NOSSAL, R. 1992. Scaling relationships for anisotropic random walks. *Journal of statistical physics* 69, 1-2, 35–53. <https://doi.org/10.1007/BF01053781>.
- GATTO, R. 2017. Saddlepoint approximation to the distribution of the total distance of the continuous time random walk. *The European Physical Journal B* 90, 12, 238. <https://doi.org/10.1140/epjb/e2017-80228-y>.
- GEORGIEV, I., KRIVANEK, J., HACHISUKA, T., NOWROUZEZAHRAI, D., AND JAROSZ, W. 2013. Joint importance sampling of low-order volumetric scattering. *ACM Trans. Graph.* 32, 6, 164–1. <https://doi.org/10.1145/2508363.2508411>.

- GOLSE, F. 2012. Recent results on the Periodic Lorentz Gas. *Nonlinear Partial Differential Equations*, 39–99. [https://doi.org/10.1007/978-3-0348-0191-1\\_2](https://doi.org/10.1007/978-3-0348-0191-1_2).
- GRANT, I. P., AND HUNT, G. 1969. Discrete space theory of radiative transfer I. Fundamentals. *Proc. R. Soc. Lond. A* 313, 1513, 183–197. <https://doi.org/10.1098/rspa.1969.0187>.
- GROSJEAN, C. 1951. The Exact Mathematical Theory of Multiple Scattering of Particles in an Infinite Medium. *Memoirs Kon. Vl. Ac. Wetensch.* 13, 36.
- GROSJEAN, C. C. 1953. Solution of the non-isotropic random flight problem in the  $k$ -dimensional space. *Physica* 19, 1-12, 29–45. [https://doi.org/10.1016/S0031-8914\(53\)80004-2](https://doi.org/10.1016/S0031-8914(53)80004-2).
- GROSJEAN, C. C. 1956. A high accuracy approximation for solving multiple scattering problems in infinite homogeneous media. *Il Nuovo Cimento* 3, 6 (Jun), 1262–1275. <https://doi.org/10.1007/BF02785007>.
- GROSJEAN, C. C. 1956. On a new approximate one-velocity theory of multiple scattering in infinite homogeneous media. *Il Nuovo Cimento* 4, 3 (Sep), 583–594. <https://doi.org/10.1007/BF02745383>.
- GROSJEAN, C. C. 1958. Multiple Isotropic Scattering in Convex Homogeneous Media Bounded by Vacuum. *Proceedings of the Second International Conference on the Peaceful Uses of Atomic Energy* 16, 413.
- GROSJEAN, C. C. 1958. Multiple Isotropic Scattering in Convex Homogeneous Media Bounded by Vacuum. Part II. Some Practical Applications. *Proceedings of the Second International Conference on the Peaceful Uses of Atomic Energy* 16, 431.
- GROSJEAN, C. C. 1963. A new approximate one-velocity theory for treating both isotropic and anisotropic multiple scattering problems. Part I. Infinite homogeneous scattering media. Tech. rep., Universiteit, Ghent.
- GROSJEAN, C. C. 1963. Recent progress in the development of a new approximate general theory of multiple scattering. In *ICES Electromagnetic Scattering*, vol. 1, 485.
- GUO, J., CHEN, Y., HU, B., YAN, L.-Q., GUO, Y., AND LIU, Y. 2019. Fractional gaussian fields for modeling and rendering of spatially-correlated media. *ACM Transactions on Graphics (TOG)* 38, 4, 45. <https://doi.org/10.1145/3306346.3323031>.
- GUTH, E., AND INÖNÜ, E. 1960. Random-Walk Interpretation and Generalization of Linear Boltzmann Equations, Particularly for Neutron Transport. *Phys. Rev.* 118, 4 (May), 899–900. <https://doi.org/10.1103/PhysRev.118.899>.
- HALL, R. 1977. Amoeboid movement as a correlated walk. *Journal of mathematical biology* 4, 4, 327–335. <https://doi.org/10.1007/BF00275081>.

- HEITZ, E., AND BELCOUR, L. 2018. A note on track-length sampling with non-exponential distributions. Research Report hal-01788593, Unity Technologies, May. <https://hal.inria.fr/hal-01788593>.
- HERSH, R. 1974. Random evolutions: a survey of results and problems. *The Rocky Mountain Journal of Mathematics* 4, 3, 443–477. <https://www.jstor.org/stable/44236397>.
- HOFFMAN, W. 1964. Wave propagation in a general random continuous medium. *Proc. Symp. Appl. Math.* 16, 117–144.
- HOOGENBOOM, E. 2008. Zero-Variance Monte Carlo Schemes Revisited. *Nucl. Sci. Eng.* 160, 1, 1–22. <https://doi.org/10.13182/NSE160-01>.
- ISHIMARU, A., AND KUGA, Y. 1982. Attenuation constant of a coherent field in a dense distribution of particles. *JOSA* 72, 10, 1317–1320. <https://doi.org/10.1364/JOSA.72.001317>.
- ISHIMARU, A. 1978. *Wave Propagation and Scattering in Random Media*. Oxford University Press.
- ISHIMARU, A. 1991. Wave propagation and scattering in random media and rough surfaces. *Proceedings of the IEEE* 79, 10, 1359–1366. <https://doi.org/10.1109/5.104210>.
- IVANOV, V. 1994. Resolvent method: exact solutions of half-space transport problems by elementary means. *Astronomy and Astrophysics* 286, 328–337.
- JAGERS, P. 1975. *Branching Processes with Biological Applications*. J. Wiley and Sons.
- JAKEMAN, E., AND PUSEY, P. 1976. A model for non-Rayleigh sea echo. *IEEE Transactions on antennas and propagation* 24, 6, 806–814. <https://doi.org/10.1109/TAP.1976.1141451>.
- JARABO, A., ALIAGA, C., AND GUTIERREZ, D. 2018. A radiative transfer framework for spatially-correlated materials. *ACM Transactions on Graphics* 37, 4, 14. <https://doi.org/10.1145/3197517.3201282>.
- JAROSZ, W., NOWROUZEZHAI, D., THOMAS, R., SLOAN, P.-P., AND ZWICKER, M. 2011. Progressive photon beams. In *ACM Transactions on Graphics (TOG)*, vol. 30, ACM, 181. <https://doi.org/10.1145/2070781.2024215>.
- JENSEN, H. W., MARSCHNER, S. R., LEVOY, M., AND HANRAHAN, P. 2001. A practical model for subsurface light transport. In *Proceedings of ACM SIGGRAPH 2001*, 511–518. <https://doi.org/10.1145/383259.383319>.
- KALLI, H., AND CASHWELL, E. 1977. Evaluation of three Monte Carlo estimation schemes for flux at a point. Tech. Rep. LA-6865-MS, Los Alamos Scientific Lab., N. Mex.(USA), Sep. <https://doi.org/10.2172/7280869>.

- KALOS, M. 1963. On the estimation of flux at a point by Monte Carlo. *Nucl. Sci. Eng. (US)* 16, 111–117. <https://doi.org/10.13182/NSE63-A26481>.
- KAREIVA, P., AND SHIGESADA, N. 1983. Analyzing insect movement as a correlated random walk. *Oecologia* 56, 2-3, 234–238. <https://doi.org/10.1007/BF00379695>.
- KELLER, J. 1962. Wave propagation in random media. *Proc. Symp. Appl. Math.* 13, 227–246.
- KIENLE, A., AND PATTERSON, M. S. 1997. Improved solutions of the steady-state and the time-resolved diffusion equations for reflectance from a semi-infinite turbid medium. *J. Opt. Soc. Am. A* 14, 1, 246–254. <https://doi.org/10.1364/JOSAA.14.000246>.
- KOSTINSKI, A. B. 2001. On the extinction of radiation by a homogeneous but spatially correlated random medium. *JOSA A* 18, 8, 1929–1933. <https://doi.org/10.1364/JOSAA.18.001929>.
- KŘIVÁNEK, J., GEORGIEV, I., HACHISUKA, T., VÉVODA, P., ŠIK, M., NOWROUZEZHAI, D., AND JAROSZ, W. 2014. Unifying points, beams, and paths in volumetric light transport simulation. *ACM Transactions on Graphics (TOG)* 33, 4, 103. <https://doi.org/10.1145/2601097.2601219>.
- KRYCKI, K. 2015. *Mathematical Modeling and Numerical Methods for Non-classical Transport in Correlated Media*. PhD thesis, RWTH Aachen University.
- KULLA, C., AND FAJARDO, M. 2012. Importance sampling techniques for path tracing in participating media. In *Computer Graphics Forum*, vol. 31, Wiley Online Library, 1519–1528. <https://doi.org/10.1111/j.1467-8659.2012.03148.x>.
- LARSEN, M. L., AND CLARK, A. S. 2014. On the link between particle size and deviations from the Beer–Lambert–Bouguer law for direct transmission. *Journal of Quantitative Spectroscopy and Radiative Transfer* 133, 646–651. <https://doi.org/10.1016/j.jqsrt.2013.10.001>.
- LARSEN, E. W., AND VASQUES, R. 2011. A generalized linear Boltzmann equation for non-classical particle transport. *Journal of Quantitative Spectroscopy and Radiative Transfer* 112, 4, 619–631. <https://doi.org/10.1016/j.jqsrt.2010.07.003>.
- LARSEN, E. W., FRANK, M., AND CAMMINADY, T. 2017. The equivalence of forward and backward nonclassical particle transport theories. *Proceedings M&C2017, Korea, April*.
- LARSEN, E. 2007. A generalized Boltzmann equation for non-classical particle transport. *Joint International Topical Meeting on Mathematics & Computation and Supercomputing in Nuclear Applications, American Nuclear Society*. on CD-ROM.
- LARSEN, E. 2010. Asymptotic Diffusion and Simplified PN Approximations for Diffusive and Deep Penetration Problems. Part 1: Theory. *Transport Theory and Statistical Physics* 39, 2-4, 110–163. <https://doi.org/10.1080/00411450.2010.531878>.

- LE CAËR, G. 2011. A new family of solvable pearson-dirichlet random walks. *Journal of Statistical Physics* 144, 1, 23–45. <https://doi.org/10.1007/s10955-011-0245-4>.
- LEVERMORE, C., WONG, J., AND POMRANING, G. 1988. Renewal theory for transport processes in binary statistical mixtures. *Journal of mathematical physics* 29, 4, 995–1004. <https://doi.org/10.1063/1.527997>.
- LIEMERT, A., AND KIENLE, A. 2017. Radiative transport equation for the Mittag-Leffler path length distribution. *Journal of Mathematical Physics* 58, 5, 053511. <https://doi.org/10.1063/1.4983682>.
- LUX, I., AND KOBLINGER, L. 1991. *Monte Carlo particle transport methods: neutron and photon calculations*, vol. 102. CRC press.
- LUX, I. 1978. General formulation of track-length-type estimators. *Nucl. Sci. Eng.* 66, 1, 121–124. <https://doi.org/10.13182/NSE78-A15195>.
- LUX, I. 1978. Unified definition of a class of Monte Carlo estimators. *Nucl. Sci. Eng.* 67, 1, 107–119. <https://doi.org/10.13182/NSE78-A27241>.
- MAJUMDAR, S. N., AND ZIFF, R. M. 2008. Universal record statistics of random walks and lévy flights. *Physical review letters* 101, 5, 050601. <https://doi.org/10.1103/PhysRevLett.101.050601>.
- MAKINE, I., VASQUES, R., AND SLAYBAUGH, R. 2018. Exact Transport Representations of the Classical and Nonclassical Simplified PN Equations. *Journal of Computational and Theoretical Transport*, 1–24. <https://doi.org/10.1080/23324309.2018.1496938>.
- MANTEGNA, R. N., AND STANLEY, H. E. 1994. Stochastic process with ultraslow convergence to a Gaussian: the truncated Lévy flight. *Physical Review Letters* 73, 22, 2946. <https://doi.org/10.1103/PhysRevLett.73.2946>.
- MARSHAK, A., AND DAVIS, A. 2005. *3D radiative transfer in cloudy atmospheres*, vol. 5117. Springer.
- MARSHAK, A., DAVIS, A., WISCOMBE, W., AND CAHALAN, R. 1997. Scale invariance in liquid water distributions in marine stratocumulus. Part II: Multifractal properties and intermittency issues. *Journal of the atmospheric sciences* 54, 11, 1423–1444.
- MARTIN, W. R. 2012. Challenges and prospects for whole-core monte carlo analysis. *Nuclear Engineering and Technology* 44, 2, 151–160. <https://doi.org/10.5516/NET.01.2012.502>.
- MAZZOLO, A., DE MULATIER, C., AND ZOIA, A. 2014. Cauchy’s formulas for random walks in bounded domains. *Journal of Mathematical Physics* 55, 8, 083308. [https://doi.org/10.1016/0306-4549\(92\)90013-2](https://doi.org/10.1016/0306-4549(92)90013-2).

- MAZZOLO, A. 2009. An invariance property of generalized Pearson random walks in bounded geometries. *Journal of Physics A: Mathematical and Theoretical* 42, 10, 105002. <https://doi.org/10.1088/1751-8113/42/10/105002>.
- MENG, J., PAPAS, M., HABEL, R., DACHSBACHER, C., MARSCHNER, S., GROSS, M. H., AND JAROSZ, W. 2015. Multi-scale modeling and rendering of granular materials. *ACM Trans. Graph.* 34, 4, 49–1. <https://doi.org/10.1145/2766949>.
- MERCADIER, N., GUERIN, W., CHEVROLIER, M., AND KAISER, R. 2009. Lévy flights of photons in hot atomic vapours. *Nature physics* 5, 8, 602. <https://doi.org/10.1038/nphys1286>.
- MISHCHENKO, M. 2008. Multiple scattering, radiative transfer, and weak localization in discrete random media: Unified microphysical approach. *Reviews of Geophysics* 46, 2. <https://doi.org/10.1029/2007RG000230>.
- MODEST, M. 2003. *Radiative heat transfer*. Academic Press.
- MOON, J., WALTER, B., AND MARSCHNER, S. 2007. Rendering discrete random media using precomputed scattering solutions. *Rendering Techniques 2007*, 231–242. <https://doi.org/10.2312/EGWR/EGSR07/231-242>.
- MÜLLER, T., PAPAS, M., GROSS, M. H., JAROSZ, W., AND NOVÁK, J. 2016. Efficient rendering of heterogeneous polydisperse granular media. *ACM Trans. Graph.* 35, 6, 168–1. <https://doi.org/10.1145/2980179.2982429>.
- MULLIKIN, T. 1968. Some probability distributions for neutron transport in a half-space. *Journal of Applied Probability* 5, 2, 357–374. <https://doi.org/10.2307/3212258>.
- MYNENI, R. B., MARSHAK, A. L., AND KNYAZIKHIN, Y. V. 1991. Transport theory for a leaf canopy of finite-dimensional scattering centers. *Journal of Quantitative Spectroscopy and Radiative Transfer* 46, 4, 259–280. [https://doi.org/10.1016/0022-4073\(91\)90091-4](https://doi.org/10.1016/0022-4073(91)90091-4).
- NOVAK, J., GEORGIEV, I., HANIKA, J., AND JAROSZ, W. 2018. Monte Carlo Methods for Volumetric Light Transport Simulation. *Computer Graphics Forum (Proceedings of Eurographics - State of the Art Reports)* 37, 2 (May). <https://doi.org/10.1111/cgf.13383>.
- OTHMER, H. G., AND HILLEN, T. 2000. The diffusion limit of transport equations derived from velocity-jump processes. *SIAM Journal on Applied Mathematics* 61, 3, 751–775. <https://doi.org/10.1137/S0036139999358167>.
- PAPANICOLAOU, G., AND KELLER, J. B. 1971. Stochastic differential equations with applications to random harmonic oscillators and wave propagation in random media. *SIAM Journal on Applied Mathematics* 21, 2, 287–305. <https://doi.org/10.1137/0121032>.

- PAPAS, M., REGG, C., JAROSZ, W., BICKEL, B., JACKSON, P., MATUSIK, W., MARSCHNER, S., AND GROSS, M. 2013. Fabricating translucent materials using continuous pigment mixtures. *ACM Transactions on Graphics (TOG)* 32, 4, 146. <https://doi.org/10.1145/2461912.2461974>.
- PELTONIEMI, J. I. 1993. Radiative transfer in stochastically inhomogeneous media. *Journal of Quantitative Spectroscopy and Radiative Transfer* 50, 6, 655–671. [https://doi.org/10.1016/0022-4073\(93\)90033-E](https://doi.org/10.1016/0022-4073(93)90033-E).
- PFEILSTICKER, K. 1999. First geometrical path length probability density function derivation of the skylight from high-resolution oxygen A-band spectroscopy: 2. Derivation of the Lévy index for the skylight transmitted by midlatitude clouds. *Journal of Geophysical Research: Atmospheres* 104, D4, 4101–4116. <https://doi.org/10.1029/1998JD200081>.
- PHARR, M., JAKOB, W., AND HUMPHREYS, G. 2016. *Physically based rendering*, 3 ed. Morgan Kaufmann, Nov.
- PIERRAT, R., AMBICHL, P., GIGAN, S., HABER, A., CARMINATI, R., AND ROTTER, S. 2014. Invariance property of wave scattering through disordered media. *Proceedings of the National Academy of Sciences* 111, 50, 17765–17770. <https://doi.org/10.1073/pnas.1417725111>.
- POGORUI, A. A., AND RODRÍGUEZ-DAGNINO, R. M. 2013. Random motion with gamma steps in higher dimensions. *Statistics & Probability Letters* 83, 7, 1638–1643. <https://doi.org/10.1016/j.spl.2013.03.011>.
- POMRANING, G. 1989. The Milne problem in a statistical medium. *Journal of Quantitative Spectroscopy and Radiative Transfer* 41, 2, 103–115. [https://doi.org/10.1016/0022-4073\(89\)90132-5](https://doi.org/10.1016/0022-4073(89)90132-5).
- PREISENDORFER, R. W. 1965. *Radiative transfer on discrete spaces*, vol. 1. Pergamon Press Oxford.
- RIEF, H., DUBI, A., AND ELPERIN, T. 1984. Track length estimation applied to point detectors. *Nucl. Sci. Eng* 87, 59. <https://doi.org/10.13182/NSE84-A17446>.
- RUKOLAINE, S. A. 2016. Generalized linear Boltzmann equation, describing non-classical particle transport, and related asymptotic solutions for small mean free paths. *Physica A: Statistical Mechanics and its Applications* 450, 205–216. <https://doi.org/10.1016/j.physa.2015.12.105>.
- RYZHIK, L., PAPANICOLAOU, G., AND KELLER, J. 1996. Transport equations for elastic and other waves in random media. *Wave motion* 24, 4, 327–370. [https://doi.org/10.1016/S0165-2125\(96\)00021-2](https://doi.org/10.1016/S0165-2125(96)00021-2).
- SATO, H., FEHLER, M. C., AND MAEDA, T. 2012. *Seismic wave propagation and scattering in the heterogeneous earth*, vol. 496. Springer.

- SAVO, R., PIERRAT, R., NAJAR, U., CARMINATI, R., ROTTER, S., AND GIGAN, S. 2017. Observation of mean path length invariance in light-scattering media. *Science* 358, 6364, 765–768. <https://doi.org/10.1126/science.aan4054>.
- SPANIER, J., AND GELBARD, E. 1969. *Monte Carlo principles and neutron transport problems*. Addison-Wesley Pub. Co.
- SPANIER, J. 1966. Two pairs of families of estimators for transport problems. *SIAM Journal on Applied Mathematics* 14, 4, 702–713. <https://doi.org/10.1137/0114059>.
- SVENSSON, T., VYNCK, K., GRISI, M., SAVO, R., BURRESI, M., AND WIERSMA, D. S. 2013. Holey random walks: Optics of heterogeneous turbid composites. *Physical Review E* 87, 2, 022120. <https://doi.org/10.1103/PhysRevE.87.022120>.
- SVENSSON, T., VYNCK, K., ADOLFSSON, E., FARINA, A., PIFFERI, A., AND WIERSMA, D. S. 2014. Light diffusion in quenched disorder: Role of step correlations. *Physical Review E* 89, 2, 022141. <https://doi.org/10.1103/PhysRevE.89.022141>.
- SWEETZ, J. E. 2018. A Monte Carlo volumetric-ray-casting estimator for global fluence tallies on GPUs. *Journal of Computational Physics* 372, 426–445. <https://doi.org/10.1016/j.jcp.2018.06.032>.
- TAINE, J., BELLET, F., LEROY, V., AND IACONA, E. 2010. Generalized radiative transfer equation for porous medium upscaling: Application to the radiative fourier law. *International Journal of Heat and Mass Transfer* 53, 19-20, 4071–4081. <https://doi.org/10.1016/j.ijheatmasstransfer.2010.05.027>.
- TORQUATO, S., AND LU, B. 1993. Chord-length distribution function for two-phase random media. *Physical Review E* 47, 4, 2950. [https://doi.org/10.1016/0306-4549\(92\)90013-2](https://doi.org/10.1016/0306-4549(92)90013-2).
- TORQUATO, S. 2016. Hyperuniformity and its generalizations. *Physical Review E* 94, 2, 022122.
- TSANG, L., CHEN, C.-T., CHANG, A. T., GUO, J., AND DING, K.-H. 2000. Dense media radiative transfer theory based on quasicrystalline approximation with applications to passive microwave remote sensing of snow. *Radio Science* 35, 3, 731–749. <https://doi.org/10.1029/1999RS002270>.
- TUCHIN, V. 2007. *Tissue Optics: Light Scattering Methods and Instruments for Medical Diagnosis*, 2nd ed. SPIE Press.
- UCHAIKIN, V., AND GUSAROV, G. 1997. Levy flight applied to random media problems. *Journal of Mathematical Physics* 38, 5, 2453–2464. <https://doi.org/10.1063/1.531959>.
- VAN DE HULST, H. 1980. *Multiple light scattering*. Academic Press.

- VASQUES, R., AND LARSEN, E. W. 2014. Non-classical particle transport with angular-dependent path-length distributions. I: Theory. *Annals of Nuclear Energy* 70, 292–300. <https://doi.org/10.1016/j.anucene.2013.12.021>.
- VASQUES, R., AND SLAYBAUGH, R. N. 2016. Simplified  $P_N$  Equations for Non-classical Transport with Isotropic Scattering. *arXiv preprint arXiv:1610.04314*. <https://arxiv.org/abs/1610.04314>.
- VASQUES, R. 2016. The nonclassical diffusion approximation to the non-classical linear Boltzmann equation. *Applied Mathematics Letters* 53, 63–68. <https://doi.org/10.1016/j.aml.2015.10.003>.
- VEACH, E. 1997. *Robust Monte Carlo Methods for Light Transport Simulation*. PhD thesis, Stanford University.
- VITALI, V., DULLA, S., RAVETTO, P., AND ZOIA, A. 2018. Comparison of Monte Carlo methods for adjoint neutron transport. *The European Physical Journal Plus* 133, 8, 317. <https://doi.org/10.1140/epjp/i2018-12132-9>.
- WANG, R. K. 2000. Modelling optical properties of soft tissue by fractal distribution of scatterers. *Journal of Modern Optics* 47, 1, 103–120. <https://doi.org/10.1080/09500340008231409>.
- WATERMAN, P. C., AND TRUPELL, R. 1961. Multiple scattering of waves. *Journal of Mathematical Physics* 2, 4, 512–537. <https://doi.org/10.1063/1.1703737>.
- WEN, B., TSANG, L., WINEBRENNER, D. P., AND ISHIMARU, A. 1990. Dense medium radiative transfer theory: comparison with experiment and application to microwave remote sensing and polarimetry. *IEEE Transactions on Geoscience and Remote Sensing* 28, 1, 46–59. <https://doi.org/10.1109/36.45744>.
- WIGNER, E. P. 1992. Mathematical problems of nuclear reactor theory. In *Nuclear Energy*. Springer, 459–474. [https://doi.org/10.1007/978-3-642-77425-6\\_30](https://doi.org/10.1007/978-3-642-77425-6_30).
- WILLIAMS, M. M. R. 1971. *Mathematical methods in particle transport theory*. Wiley.
- WILLIAMS, M. 1974. *Random processes in nuclear reactors*. Pergamon.
- WILLIAMS, M. 1997. Radiation transport in random slabs with binomial statistics. *Transport Theory and Statistical Physics* 26, 4-5, 619–628. <https://doi.org/10.1080/00411459708017933>.
- WITT, A. N., AND GORDON, K. D. 1996. Multiple scattering in clumpy media. I. Escape of stellar radiation from a clumpy scattering environment. *The Astrophysical Journal* 463, 681. <https://doi.org/10.1086/177282>.
- WITT, A. N., AND GORDON, K. D. 2000. Multiple scattering in clumpy media. II. Galactic environments. *The Astrophysical Journal* 528, 2, 799. <https://doi.org/10.1086/308197>.

- WRENNINGE, M., VILLEMIN, R., AND HERY, C. 2017. Path traced subsurface scattering using anisotropic phase functions and non-exponential free flights. Tech. Rep. 17-07, Pixar. <https://graphics.pixar.com/library/PathTracedSubsurface>.
- ZABURDAEV, V., DENISOV, S., AND KLAFTER, J. 2015. Lévy walks. *Reviews of Modern Physics* 87, 2, 483. <https://doi.org/10.1103/RevModPhys.87.483>.
- ZOIA, A., DUMONTEIL, E., AND MAZZOLO, A. 2011. Collision densities and mean residence times for d-dimensional exponential flights. *Physical Review E* 83, 4, 041137. <https://doi.org/10.1103/PhysRevE.83.041137>.

## A Gamma-2 Flux Derivation in 3D

The plane-geometry kernel  $K_\phi(x)$  producing collided flux from the collision rate density in 3D transport with isotropic scattering is

$$K_\phi(x) = \frac{c}{2} \int_0^1 X_c(|x|/\mu) \frac{1}{\mu} d\mu, \quad (156)$$

which for Gamma-2 transport is

$$K_\phi(x) = \frac{c}{2} \left( e^{-|x|} + E_1(|x|) \right). \quad (157)$$

Mathematica is able to compute the collided flux from a collision rate density given by a diffusion mode  $C(x) = e^{-|x|/v}$ ,

$$\begin{aligned} \int_{-\infty}^{\infty} e^{-|t|/v} K_\phi(t-x) dt &= cvE_1(|x|) \\ &+ \frac{cve^{-\frac{|x|}{v}} \left( -e^{\left(\frac{1}{v}-1\right)|x|} + (v^2-1) \coth^{-1}(v) + v \right)}{v^2-1} \\ &+ \frac{1}{2} cve^{-\frac{|x|}{v}} \left[ -E_1 \left( \left(1 - \frac{1}{v}\right) |x| \right) - e^{\frac{2|x|}{v}} E_1 \left( \frac{(v+1)|x|}{v} \right) \right]. \end{aligned} \quad (158)$$

Performing the convolution in Eq. 158 in the frequency domain using

$$\int_{-\infty}^{\infty} e^{-|t|/v} e^{izx} dx = \frac{2v}{1+v^2z^2} \quad (159)$$

and

$$\int_{-\infty}^{\infty} K_\phi(x) e^{izx} dx = c \left( \frac{1}{z^2+1} + \frac{\tan^{-1}(z)}{z} \right) \quad (160)$$

we find that the convolution is given by the following Fourier inversion

$$\begin{aligned} \int_{-\infty}^{\infty} e^{-|t|/v} K_\phi(t-x) dt \\ = \frac{1}{2\pi} \int_{-\infty}^{\infty} \frac{2v}{1+v^2z^2} c \left( \frac{1}{z^2+1} + \frac{\tan^{-1}(z)}{z} \right) e^{-izx} dx. \end{aligned} \quad (161)$$

Given that the convolution of the two diffusion terms is simple

$$\frac{1}{2\pi} \int_{-\infty}^{\infty} \frac{2v}{1+v^2z^2} c \left( \frac{1}{z^2+1} \right) e^{-izx} dx = \frac{cv \left( e^{-|x|} - v e^{-\frac{|x|}{v}} \right)}{1-v^2} \quad (162)$$

we can solve to find that the Fourier inversion of the arctan term is therefore

$$\begin{aligned} Z_{pl}(x, v) &= \frac{1}{2\pi} \int_{-\infty}^{\infty} \frac{1}{1+v^2z^2} \left( \frac{\tan^{-1}(z)}{z} \right) e^{-izx} dx \\ &= \frac{1}{2} \coth^{-1}(v) e^{-\frac{|x|}{v}} + \frac{E_1(|x|)}{2} - \frac{1}{4} e^{-\frac{|x|}{v}} E_1 \left( \left( 1 - \frac{1}{v} \right) |x| \right) \\ &\quad - \frac{1}{4} e^{\frac{|x|}{v}} E_1 \left( \frac{(v+1)|x|}{v} \right). \end{aligned} \quad (163)$$

Using the plane-to-point transform [Case et al. 1953]

$$\phi_{pt}(r) = -\frac{1}{2\pi r} \frac{d\phi_{pl}(x)}{dx} \Big|_{x=r} \quad (164)$$

we also have the spherical-geometry equivalent,

$$\begin{aligned} Z_{pt}(r, v) &= \mathcal{F}_3^{-1} \left\{ \frac{\tan^{-1} z}{z} \frac{1}{1+(zv)^2} \right\} = \\ &= \frac{e^{-\frac{r}{v}} \left( -E_1 \left( r \left( 1 - \frac{1}{v} \right) \right) + e^{\frac{2r}{v}} E_1 \left( r \left( 1 + \frac{1}{v} \right) \right) + 2 \coth^{-1}(v) \right)}{8\pi v r}. \end{aligned} \quad (165)$$

With these results we are able to express the scalar flux about the correlated-emission isotropic plane source (Eq. 80)

$$\phi_c(x) = \frac{E_1(|x|)}{2} + \frac{e^{-\sqrt{1-c}|x|}}{2\sqrt{1-c}} + \frac{c}{1-c} Z_{pl}(x, \frac{1}{\sqrt{1-c}}) \quad (166)$$

and the scalar flux about the correlated-emission isotropic point source, Eq. 75

$$\phi_c(r) = \frac{e^{-r}}{4\pi r^2} + \frac{e^{-r\sqrt{1-c}}}{4\pi r} + \frac{c}{1-c} Z_{pt}(r, \frac{1}{\sqrt{1-c}}) \quad (167)$$

## B Nonexponential Monte Carlo Estimation: Additional Details

### B.1 Collision / Track-Length Duality and Joint Estimation

In Section 3, we found two complementary pairs of estimators, two of the collision type and two of the track-length type. In some sense, the collision estimator most naturally estimates collision rate, and the track-length estimator most naturally estimates flux. This echoes the duality of flux creating collisions and collisions creating flux in linear transport theory. Each estimator can compute its primal quantity locally in the smaller phase space with no memory (track-length for flux and collision rate for collision), while requiring the memory variable  $s$  to compute the complementary quantity. The

advantages of both can be realized over the same random walk by having each contribute separately to distinct flux-proportional and collision-proportional tallies.

It is natural to ponder whether or not there exist variants of each estimator that estimate the other quantity in a memory-free way, and indeed there are (with a few restrictions). This can be achieved by sampling free-path lengths from non-analog PDFs, and essentially moves the memory-dependent calculation to a *particle weight*  $W$ , which still ends up in the score. This would seem to offer little advantage in the case of the collision estimator, but is more interesting in the case of track-length estimation.

For completeness, and to begin with the simpler case, let us first consider how this would work for the collision estimator. Consider correlated free-path lengths that are sampled from  $p_u(s)$  instead of  $p_c(s)$ . Collisions will now occur in proportion to the flux, due to the definition of  $p_u(s)$ . A collision estimator scoring  $W\langle s_c \rangle$  is then a memory-free unbiased collision estimator of the flux. The weight factor begins the walk at  $W = 1$  and updates prior to each collision using

$$W \leftarrow \left( W \frac{p_c(s)}{p_u(s)} = W \frac{\Sigma_{tc}(\mathbf{x}, \vec{\omega}, E, s)}{\langle s_c \rangle} \right). \quad (168)$$

It is clear that we have simply moved the memory-dependent term  $\Sigma_{tc}(s)$  into the weight factor  $W$ .

For the case of track-length estimation of collision-rate, Heitz and Belcour [2018] noted that sampling track-lengths proportional to the derivative of the free-path distribution (provided it is monotonically decreasing) and applying a normalization weight (a constant) to each track-length estimate is an unbiased estimator for the free-path distribution and, therefore, the collision rate density. Again, the memory calculation is moved into a weight factor update at each such non-analog free-path sampling, but now the advantage is that the score along the track-length is a constant times the length and the integral of the cross-section is avoided.

Employing either of these path-length biasings successively in creating a full random walk is inadvisable, due to the weight fluctuations that could occur and chain together. However, a modified walk of the kind described by Sweezy [2018] could be adapted here as follows. An analog walk is sampled as above, but its track lengths and collision sites are not used to score. Instead, at each source vertex and non-terminating collision vertex of the analog walk,  $N$  scoring tracks, each with weight factors  $1/N$  are sampled using the phase function and non-analog free-path distributions just described (for the corresponding origin type). By spawning the scoring tracks from the vertices of the analog walk, we both solve the same integral equation as would be solved by scoring from the walk itself, and contributions of all scattering orders are included. Accumulated weight-factor fluctuations are, however, avoided by building the primary walk with analog free-path sampling. Applying this method for track-length estimation of collision rate involves temporary weight factors for each scoring track, which depend on  $s$  and scale the track-length scores. These weights are then discarded after scoring and the walk continues in the analog fashion to the next vertex.

The same idea can extend the collision-rate-density-estimation methods of the track-length type called “photon beams” by Jarosz et al. [Jarosz et al. 2011; Novak et al. 2018] for GRT. These algorithms sample and store a number of particle histories (in the forward direction) into a data structure that is later used to share these calculations over millions of next-event estimations through a virtual camera aperture and onto the pixels comprising an image of light scattering within participating media, such as fog or tissue. The next-event calculations are of the back-projection angular flux type [Dunn 1985] and are combined with biased kernel density estimation. The extension just described would yield memory-free track-length estimates across each density-estimation kernel, avoiding the cross-section integrals otherwise required to estimate the density of collisions that send light into the direction of the camera’s aperture.

## B.2 Non-Analog Games

It is often advantageous to deviate from the analog walk by altering the probabilities of absorption, scattering angle, and free-path length sampling to reduce variance and improve performance [Lux and Koblinger 1991; Hoogenboom 2008]. The most common and basic of such schemes utilize the classical particle weight concept, with weight corrections calculated in the usual fashion.

Implicit capture in GRT remains unchanged, multiplying the particle weight  $W$  by  $c(\mathbf{x})$  at each collision and applying additional weight changes if Russian roulette is used to terminate the walk. Collision and track-length scores are then scaled, per collision and track segment, by the current particle weight  $W_i$ . Likewise, angle biasing can use non-analog phase functions  $P'$  by adopting a weight factor

$$W \leftarrow W \times \frac{P(\vec{\omega}_i, \vec{\omega}_{i+1})}{P'(\vec{\omega}_i, \vec{\omega}_{i+1})} \quad (169)$$

prior to the next score. Path-length biasing from a non-analog PDF  $p'(s)$  requires a similar correction for the collision estimators prior to scoring

$$W \leftarrow W \frac{p_-(s)}{p'(s)}. \quad (170)$$

For non analog free-path sampling  $p'(s)$  (other than the forms previously discussed), the track-length estimators both become memory dependent and require changes, similar in derivation to the case presented above, which we skip for brevity.

## B.3 Estimation at a Point

Next-event estimation (NEE) at a point in GRT takes on four forms, generalizing the classically equivalent estimators. In all cases the geometry factor of  $1/r^2$  leads to an estimator of unbounded variance in 3D space [Kalos 1963] and should be avoided using equiangular sampling or similar approaches that remove the singularity [Kalli and Cashwell 1977; Rief et al. 1984; Kulla and Fajardo 2012; Georgiev et al. 2013]. The collision-rate expected value estimate at  $\mathbf{x}$  from a correlated-origin walk vertex  $\mathbf{x}_c$

is

$$\frac{p_c(\|\mathbf{x} - \mathbf{x}_c\|)P(\vec{\omega}_i, \frac{\mathbf{x} - \mathbf{x}_c}{\|\mathbf{x} - \mathbf{x}_c\|})}{\|\mathbf{x} - \mathbf{x}_c\|^2}. \quad (171)$$

For uncorrelated-origins,  $p_c$  is replaced with  $p_u$ . For flux expected value estimates, the free-path distributions  $p_c(s)$ , and  $p_u(s)$  change to transmittances  $X_c(s)$  and  $X_u(s)$  respectively for correlated and uncorrelated origins. Integration of these estimators along track-lengths yields the respective generalizations.

#### B.4 Dwivedi Guiding

Analog walks are particularly ineffective at estimating extremely low values, such as shielding calculations through very thick slabs. A highly effective method for guiding the walk in this case toward a zero-variance estimator for penetration through the slab is to assume an approximate importance function of escape at each optical depth  $z$  with translational invariance of the form [Dwivedi 1982]

$$I_e(z) = e^{-z/v_0} \quad (172)$$

where  $v_0 > 1$  is the largest discrete eigenvalue for the transport kernel [Case and Zweifel 1967]. We found this approach to generalize for GRT, provided, at least,  $p_c(s)$  has bounded moments of all orders, by noting that angle selection, assuming an exponential escape probability for exiting a plane-parallel system after entering a collision at depth  $z$ , is the normalization of

$$\phi_{v_0}(\mu) = \frac{1}{2}c \int_0^\infty p_c(t) \exp\left(\frac{\mu}{v_0}t\right) dt, \quad (173)$$

where  $\mu$  is the direction cosine to the depth axis. For the Gamma-2 free path distribution  $p_c(s) = e^{-s}$  we find

$$\phi_{v_0}(\mu) = \frac{c}{2} \left( \frac{v_0}{v_0 - \mu} \right)^2, \quad (174)$$

which is normalized

$$\int_{-1}^1 \phi_{v_0}(\mu) d\mu = 1 \quad (175)$$

provided  $v_0 = 1/\sqrt{1-c}$ . We found it practical to sample free-paths and angles using this generalized Case eigenmode and found a five order of magnitude reduction in variance for the transmission of normally-incident beam illumination through a 20 mean-free-path thick slab with single-scattering albedo  $c = 0.7$  compared to the analog walk. We postpone the details, in part, because in Part 4 of this work we present the perfectly zero-variance walk for the half space related to this approach, which will be a better forum for highlighting how the Dwivedi method changes in GRT.

For the power-law free-path distributions discussed above, the normalization of this angular importance distribution is impossible for  $\mu/v_0 > 0$ , so the method would only apply to angle selection in one hemisphere. In the directions where the exponential importance increases, the integral of  $p_c(s)I_e(z(s))$  is unbounded. Clamping  $I_e(z)$  outside of the slab would be required, which complicates the sampling procedure, but may be practical in some cases.

## B.5 Sampling Free-Path Distribution Tails

To sample the tail of some PDF  $p(s)$  starting at  $p_0$ , where the sampling procedure for all of  $p(s)$  used the single-random-variable CDF-inversion trick, we can simply remap the range of the random number using the CDF to exclude the range  $[0, p_0]$ , which is necessarily possible because we needed to know that CDF to invert it for the standard sampling procedure. This yields a range of uniform random number  $\xi \in [a, 1]$  (or possibly  $\xi \in [0, a]$ ), which, when passed to the sampling procedure for  $p(s)$ , yields  $s \in [p_0, \infty]$ , from which we subtract  $p_0$ .

For free-path distributions, such as Mittag-Leffler, where the CDF inversion method is not possible [Fulger et al. 2008], alternative methods will be required.